

Critical point search and linear response theory for computing electronic excitation energies of molecular systems. Part I: General framework, application to Hartree-Fock and DFT

Laura Grazioli, Yukuan Hu, and Eric Cancès

CERMICS, Ecole des Ponts - Institut Polytechnique de Paris and Inria,
6-8 avenue Blaise Pascal, Cité Descartes, 77455 Marne-la-Vallée, France

June 23, 2025

Abstract

Computing excited states of many-body quantum Hamiltonians is a fundamental challenge in computational physics and chemistry, with state-of-the-art methods broadly classified into variational (critical point search) and linear response approaches. This article introduces a unified framework based on the Kähler manifold formalism, which naturally accommodates both strategies for a wide range of variational models, including Hartree-Fock, CASSCF, Full CI, and adiabatic TDDFT. In particular, this formalism leads to a systematic and straightforward way to obtain the final equations of linear response theory for nonlinear models, which provides, in the case of mean-field models (Hartree-Fock and DFT), a simple alternative to Casida’s derivation. We detail the mathematical structure of Hamiltonian dynamics on Kähler manifolds, establish connections to standard quantum chemistry equations, and provide theoretical and numerical comparisons of excitation energy computation schemes at the Hartree-Fock level.

1 Introduction

Computing excited states of many-body quantum Hamiltonians is one of the biggest challenges in computational physics and chemistry¹.

The main approaches for computing approximate excited states can be classified into two categories:

1. variational or bivariational methods: computation of critical points of energy functionals on differentiable manifolds or algebraic varieties. This category encompasses state-specific and state-averaged methods^{2–8};
2. methods based on linear response theory. Linear-response Hartree-Fock^{9–15} (LR-HF), Complete Active Space Self-Consistent Field^{16–19} (LR-CASSCF), time-dependent density functional theory^{20–25} (LR-TDDFT), and equation-of-motion coupled cluster^{26–34} (EOM-CC) fall into this category.

All these approaches coincide for the reference electronic Schrödinger equation set on the continuous position space $\bigwedge^N L^2(\mathbb{R}^3; \mathbb{C}^2)$, as well as for the Full Configuration Interaction (FCI) approximation^{35,36}, but differ when further approximations are made. This article

aims at providing a unified and compact framework covering critical point search (CP) and linear response theory (LR) from a theoretical viewpoint.

We will use the Kähler manifold formalism allowing one to conveniently formulate CP and LR for any variational model, including any variant of HF (restricted, unrestricted, general, restricted open-shell), CASSCF, and FCI methods, in a unified and compact framework. It also applies to adiabatic TDDFT^{37,38}, as this method has an intrinsic Hamiltonian Kähler structure, although it is not a variational approximation of the reference electronic Schrödinger equation. We will concentrate on the FCI and HF theories in this study. The cases of more advanced variational approximations such as CASSCF³⁹ and bivariational approximations such as CC^{40–42} will be dealt with in a future work.

If \mathcal{M} is a Kähler manifold (the definition and properties of this mathematical structure will be recalled in Section 2), and $\mathcal{E} : \mathcal{M} \rightarrow \mathbb{R}$ an energy functional over \mathcal{M} , the Hamiltonian Kähler dynamics is defined as

$$\frac{dx}{dt}(t) = J_{x(t)} \text{grad}_{\mathcal{M}} \mathcal{E}(x(t)), \quad (1)$$

where $\text{grad}_{\mathcal{M}} \mathcal{E}(x)$ is the Riemannian gradient of \mathcal{E} at point $x \in \mathcal{M}$, and J_x the so-called symplectic operator at point x . The critical points (steady states) therefore satisfy

$$\text{grad}_{\mathcal{M}} \mathcal{E}(x_*) = 0. \quad (2)$$

The CP approach for computing excitation energies consists in:

1. finding critical points x_0, x_1, x_2, \dots of \mathcal{E} on \mathcal{M} that can be identified with approximate ground and excited states, labelled in such a way that $\mathcal{E}(x_0) \leq \mathcal{E}(x_1) \leq \mathcal{E}(x_2) \leq \dots$;
2. computing the k -th excitation energy as the difference

$$\omega_k^{\text{CP}} := \mathcal{E}(x_k) - \mathcal{E}(x_0), \quad (3)$$

between the energies of the approximation x_k of the k -th excited state and the approximation x_0 of the ground state, i.e., the (presumably) global minimum of \mathcal{E} on \mathcal{M} .

Step 1 is quite involved. Indeed, in contrast with linear models such as FCI, not all critical points of nonlinear models such as HF or CASSCF are suitable approximations of ground or excited states of the reference electronic Schrödinger equation. In general, the energy functional \mathcal{E} can have many spurious critical points on \mathcal{M} . Worse still, there can be mismatch between the k -th excited states and the critical points with a Morse index k , i.e., critical points where the Riemannian Hessian has exactly k negative eigenvalues. This phenomenon is illustrated on a 2D toy model in Fig. 1, as well as on an H_4 molecule in Section 5.2. In Ref.⁴³, Lewin introduced a nonlinear min-max characterization of physically-relevant critical points for CASSCF with no internal orbitals. In Ref.⁴⁴, an algorithm for computing CASSCF approximations of first excited states based on this characterization was proposed and tested on an H_2 molecule.

In LR, the excitation energies are identified with the resonant energies of the linearized dynamics around the global minimum x_0 of \mathcal{E} on \mathcal{M} . This dynamics is given by

$$\frac{dy}{dt}(t) = J_{x_0} \text{Hess}_{\mathcal{M}} \mathcal{E}(x_0) y(t), \quad (4)$$

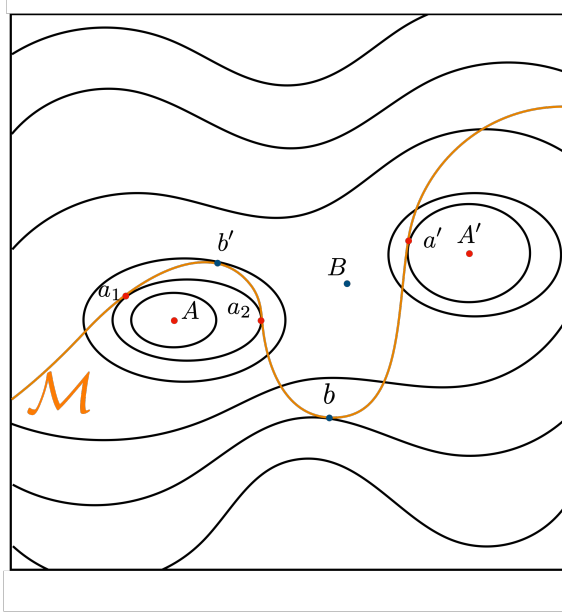


Figure 1: Contour of a 2D function $E : (0, 1) \times (0, 1) \rightarrow \mathbb{R}$ with one global minimizer (A), one local, non-global minimizer (A') and one saddle point with Morse index 1 (B). The restriction \mathcal{E} of this function to the one-dimensional manifold \mathcal{M} (indicated by the orange curve) has 3 global minimizers (a_1 , a_2 , a'), 0 local, non-global, minimizers, and 2 critical points (b , b') with a Morse index 1, which are also local maxima since \mathcal{M} is one-dimensional. The points a_1 and a_2 can be considered as reasonable approximations of A , a' as a reasonable approximation of A' , b as a reasonable approximation of B . The point b' is a spurious critical point, which does not approximate well any saddle point of E .

where $\text{Hess}_{\mathcal{M}}\mathcal{E}(x_0)$ is the Riemannian Hessian of \mathcal{E} at x_0 . Under a nondegeneracy assumption, it follows that the approximate excitation energies ω_k^{LR} computed by LR are in fact the symplectic eigenvalues of $\text{Hess}_{\mathcal{M}}\mathcal{E}(x_0)$:

$$\{\omega_k^{\text{LR}}\}_{1 \leq k \leq \dim_{\mathbb{C}}(\mathcal{M})} := \{\text{symplectic eigenvalues of } \text{Hess}_{\mathcal{M}}\mathcal{E}(x_0)\}. \quad (5)$$

This approach provides a systematic and conceptually simple way to derive linear-response approximations to excitation energies for any variational model with Kähler structure.

In Section 2, we present the abstract framework of Hamiltonian dynamics on a generic Kähler manifold, and define precisely the mathematical objects arising in the fundamental Eqs. (1)-(5). In Section 3, we consider the specific case of Hamiltonian dynamics on Grassmann manifolds

$$\mathcal{M} = \text{Gr}_{\mathbb{C}}(r, n) := \{\gamma \in \mathbb{C}_{\text{herm}}^{n \times n} \mid \gamma^2 = \gamma, \text{Tr}(\gamma) = r\}, \quad (6)$$

allowing one to deal with FCI (or more generally any linear Schrödinger or Liouville equation on a finite-dimensional state-space), HF, and adiabatic TDDFT. In Section 3.1, we describe the Kähler structure of Grassmann manifolds. In Section 3.2, we give more explicit formulations of Eqs. (1)-(5) in the special case when \mathcal{M} is a Grassmann manifold and apply this formalism to a molecular system with N_b atomic spin-orbitals and N electrons. In Section 3.3, we deal with the FCI framework, where $n = \binom{N_b}{N}$, $r = 1$, $\Gamma \in \text{Gr}_{\mathbb{C}}(1, n) \subset \mathbb{C}_{\text{herm}}^{n \times n}$ represents the N -body density matrix, and the energy functional

\mathcal{E} is linear, i.e., $\mathcal{E}(\Gamma) = \text{Tr}(H\Gamma)$ with $H \in \mathbb{C}_{\text{herm}}^{n \times n}$ the Hamiltonian matrix (specified later). We show that Eq. (1) is then equivalent to the time-dependent Schrödinger equation:

$$\widehat{\Gamma}(t) = |\Psi(t)\rangle\langle\Psi(t)| \quad \text{with} \quad i\frac{d\Psi}{dt}(t) = \widehat{H}\Psi(t), \quad \|\Psi(t)\| = 1,$$

and that Eq. (2) is equivalent to the time-independent Schrödinger equation:

$$\widehat{\Gamma} = |\Psi\rangle\langle\Psi| \quad \text{with} \quad \widehat{H}\Psi = E\Psi, \quad \|\Psi\| = 1.$$

We also show that, denoting by E_0 the ground-state energy of \widehat{H} , by Ψ_\star a normalized ground state, and by $\widehat{\Gamma}_\star = |\Psi_\star\rangle\langle\Psi_\star|$, the symplectic eigenvalues of $\text{Hess}_{\mathcal{M}}\mathcal{E}(\Gamma_\star)$ coincide with the eigenvalues of $(\widehat{H} - E_0)|_{\Psi_\star^\perp}$. It follows that, as expected,

$$\omega_k^{\text{CP-FCI}} = \omega_k^{\text{LR-FCI}} = E_k - E_0,$$

where E_k is the energy of the k -th FCI excited state. In Section 3.4, we consider the case of mean-field models, including HF and adiabatic TDDFT. In this case, $n = N_b$, $r = N$, $\gamma \in \mathbb{C}_{\text{herm}}^{N_b \times N_b}$ represents the one-body reduced density matrix (1-RDM), and the energy functional \mathcal{E} is nonlinear. Eq. (1) is then equivalent to the time-dependent HF (TDHF) or adiabatic TDDFT equations, Eq. (2) to the usual HF or Kohn-Sham equations, and Eq. (5) leads to a straightforward derivation of the final equation providing single excitation energies. Recall that this equation is usually inferred from Casida's equations of LR-TDHF or LR-TDDFT²³. In Section 4, we make use of the compact formalisms (1)-(5) to provide a theoretical comparison of the electronic excitation energy computation methods based on CP on the one-hand and LR on the other hand, at the UHF level of theory in the weakly interacting regime. More precisely, we consider a family of energy functionals of the form

$$\mathcal{E}(\lambda, \gamma) := \text{Tr}(h\gamma) + \frac{\lambda}{2}\text{Tr}(G(\gamma)\gamma) \quad \text{on} \quad \mathcal{M} = \text{Gr}_{\mathbb{C}}(N, N_b),$$

where $h \in \mathbb{C}_{\text{herm}}^{N_b \times N_b}$ and $G : \mathbb{C}_{\text{herm}}^{N_b \times N_b} \rightarrow \mathbb{C}_{\text{herm}}^{N_b \times N_b}$ combines the Coulomb and exchange terms (defined later). We compare the UHF electronic excitation energies $\omega_k^{\text{HF,CP}}(\lambda)$ and $\omega_k^{\text{HF,LR}}(\lambda)$ obtained by CP and LR respectively for small values of λ . In Section 5, we report numerical results supporting our theoretical analysis.

2 Hamiltonian dynamics on Kähler manifolds

In this section, we intend to provide a brief introduction to Kähler manifolds and associated Hamiltonian dynamics. We refer interested readers to e.g., the monographs⁴⁵⁻⁴⁷.

A Kähler manifold is a complex manifold \mathcal{M} of complex dimension $n = \dim_{\mathbb{C}}(\mathcal{M})$, endowed with a positive definite Hermitian form $\langle \bullet, \bullet \rangle_\bullet$, which allows one to endow $\mathcal{M}_{\mathbb{R}}$ (the manifold \mathcal{M} seen this time as a real $2n$ -dimensional manifold) with

1. a Riemannian structure with metric defined by

$$\forall u, v \in T_x\mathcal{M}_{\mathbb{R}}, \quad g_x(u, v) := \text{Re}(\langle u, v \rangle_x);$$

2. a symplectic structure with symplectic form defined by

$$\forall u, v \in T_x\mathcal{M}_{\mathbb{R}}, \quad \omega_x(u, v) := \text{Im}(\langle u, v \rangle_x).$$

The symplectic operator $J_x : T_x \mathcal{M}_{\mathbb{R}} \rightarrow T_x \mathcal{M}_{\mathbb{R}}$ is defined by

$$\forall u, v \in T_x \mathcal{M}_{\mathbb{R}}, \quad g_x(u, v) = \omega_x(u, J_x v).$$

It is easy to check that, for any $u, v \in T_x \mathcal{M}_{\mathbb{R}}$,

$$g_x(J_x u, J_x v) = g_x(u, v), \quad \omega_x(J_x u, J_x v) = \omega_x(u, v), \quad \omega_x(u, v) = -g_x(u, J_x v). \quad (7)$$

Let $\mathcal{E} : \mathcal{M}_{\mathbb{R}} \rightarrow \mathbb{R}$ be a smooth real-valued function on $\mathcal{M}_{\mathbb{R}}$. We denote respectively by

$$d\mathcal{E} : \mathcal{M}_{\mathbb{R}} \rightarrow T^* \mathcal{M}_{\mathbb{R}} \quad \text{and} \quad \text{grad}_{\mathcal{M}} \mathcal{E} : \mathcal{M}_{\mathbb{R}} \rightarrow T \mathcal{M}_{\mathbb{R}}$$

the differential of \mathcal{E} and its Riemannian gradient. For each $x \in \mathcal{M}_{\mathbb{R}}$, $d\mathcal{E}(x)$ is the unique \mathbb{R} -linear form on $T_x \mathcal{M}_{\mathbb{R}}$ such that for any smooth path $c : [-1, 1] \rightarrow \mathcal{M}_{\mathbb{R}}$ drawn on $\mathcal{M}_{\mathbb{R}}$ satisfying $c(0) = x$ and $\dot{c}(0) = v \in T_x \mathcal{M}_{\mathbb{R}}$,

$$\mathcal{E}(c(t)) = \mathcal{E}(x) + t d\mathcal{E}(x)(v) + o(t),$$

and $\text{grad}_{\mathcal{M}} \mathcal{E}(x)$ the unique vector of $T_x \mathcal{M}_{\mathbb{R}}$ such that

$$\forall v \in T_x \mathcal{M}_{\mathbb{R}}, \quad d\mathcal{E}(x)(v) = g_x(\text{grad}_{\mathcal{M}} \mathcal{E}(x), v).$$

The Hamiltonian dynamics on the symplectic manifold $(\mathcal{M}_{\mathbb{R}}, J_{\bullet})$ is defined by

$$\frac{dx}{dt}(t) = J_{x(t)} \text{grad}_{\mathcal{M}} \mathcal{E}(x(t)). \quad (8)$$

The equilibrium points (steady states) satisfy

$$\text{grad}_{\mathcal{M}} \mathcal{E}(x_{\star}) = 0 \quad (9)$$

and the LR around an equilibrium point x_{\star} consists in studying the linearized dynamics around x_{\star} given by

$$\frac{dy}{dt}(t) = J_{x_{\star}} \text{Hess}_{\mathcal{M}} \mathcal{E}(x_{\star}) y(t), \quad (10)$$

where $\text{Hess}_{\mathcal{M}} \mathcal{E}(x_{\star}) : T_{x_{\star}} \mathcal{M}_{\mathbb{R}} \rightarrow T_{x_{\star}} \mathcal{M}_{\mathbb{R}}$ is the Riemannian Hessian of \mathcal{E} at x_{\star} . Recall that $\text{Hess}_{\mathcal{M}} \mathcal{E}(x_{\star})$ is the unique symmetric \mathbb{R} -linear operator on $T_{x_{\star}} \mathcal{M}_{\mathbb{R}}$ such that for all smooth paths $c : [-1, 1] \rightarrow \mathcal{M}_{\mathbb{R}}$ satisfying $c(0) = x_{\star}$ and $\dot{c}(0) = v \in T_{x_{\star}} \mathcal{M}_{\mathbb{R}}$,

$$\mathcal{E}(c(t)) = \mathcal{E}(x_{\star}) + \frac{t^2}{2} g_{x_{\star}}(v, \text{Hess}_{\mathcal{M}} \mathcal{E}(x_{\star}) v) + o(t^2),$$

and that symmetric means

$$\forall u, v \in T_{x_{\star}} \mathcal{M}_{\mathbb{R}}, \quad g_{x_{\star}}(u, \text{Hess}_{\mathcal{M}} \mathcal{E}(x_{\star}) v) = g_{x_{\star}}(\text{Hess}_{\mathcal{M}} \mathcal{E}(x_{\star}) u, v).$$

Eq. (10) is a Hamiltonian dynamics on the symplectic space $(T_{x_{\star}} \mathcal{M}_{\mathbb{R}}, J_{x_{\star}})$ with quadratic Hamiltonian

$$\mathfrak{h}_{x_{\star}}(y) := \frac{1}{2} g_{x_{\star}}(y, \text{Hess}_{\mathcal{M}} \mathcal{E}(x_{\star}) y).$$

Let (u_1, \dots, u_n) be an orthonormal basis of $T_{x_{\star}} \mathcal{M}$ for $\langle \bullet, \bullet \rangle_{x_{\star}}$, i.e., a family of n vectors of $T_{x_{\star}} \mathcal{M}$ such that

$$\langle u_j, u_{j'} \rangle_{x_{\star}} = \delta_{jj'},$$

and $\mathcal{X} := \text{Span}_{\mathbb{R}}(u_1, \dots, u_n)$ the n -dimensional real-vector space spanned by the u_j 's. We have

$$T_{x_*} \mathcal{M}_{\mathbb{R}} = \mathcal{X} \oplus_{\mathbb{R}} (J_{x_*} \mathcal{X}),$$

and we infer from Eq. (7) that in the basis $(u_1, \dots, u_n, J_{x_*} u_1, \dots, J_{x_*} u_n)$ of $T_{x_*} \mathcal{M}_{\mathbb{R}}$, g_{x_*} is represented by the identity matrix I_{2n} , J_{x_*} by the skew symmetric matrix

$$J := \begin{pmatrix} 0 & -I_n \\ I_n & 0 \end{pmatrix}.$$

The Hessian matrix $\text{Hess}_{\mathcal{M}} \mathcal{E}(x_*)$ is represented by the real symmetric matrix

$$\mathfrak{H}_* := \begin{pmatrix} H^{\text{rr}} & H^{\text{ri}} \\ H^{\text{ir}} & H^{\text{ii}} \end{pmatrix} \in \mathbb{R}_{\text{sym}}^{2n \times 2n} \quad (11)$$

with entries

$$[H^{\text{rr}}]_{jj'} := g_{x_*}(u_j, \text{Hess}_{\mathcal{M}} \mathcal{E}(x_*) u_{j'}), \quad (12)$$

$$[H^{\text{ri}}]_{jj'} := g_{x_*}(u_j, \text{Hess}_{\mathcal{M}} \mathcal{E}(x_*) (J_{x_*} u_{j'})), \quad (13)$$

$$[H^{\text{ir}}]_{jj'} := g_{x_*}(J_{x_*} u_j, \text{Hess}_{\mathcal{M}} \mathcal{E}(x_*) u_{j'}), \quad (14)$$

$$[H^{\text{ii}}]_{jj'} := g_{x_*}(J_{x_*} u_j, \text{Hess}_{\mathcal{M}} \mathcal{E}(x_*) (J_{x_*} u_{j'})). \quad (15)$$

If x_* is a nondegenerate local minimizer of \mathcal{E} on $\mathcal{M}_{\mathbb{R}}$, then the matrix \mathfrak{H}_* is real symmetric positive definite (SPD). According to Williamson's theorem⁴⁸, there exists a symplectic matrix $S \in \mathbb{R}^{2n \times 2n}$ (i.e., a matrix in $\mathbb{R}^{2n \times 2n}$ such that $S^T J S = J$) such that

$$S^T \mathfrak{H}_* S = \begin{pmatrix} \Omega & 0 \\ 0 & \Omega \end{pmatrix} \quad \text{with} \quad \Omega := \text{diag}(\omega_1^{\text{LR}}, \dots, \omega_n^{\text{LR}}), \quad 0 < \omega_1^{\text{LR}} \leq \dots \leq \omega_n^{\text{LR}}. \quad (16)$$

The ω_j^{LR} 's are called the symplectic eigenvalues of \mathfrak{H}_* . It is easy to show that these quantities are independent of the chosen orthonormal basis (u_1, \dots, u_n) of $T_{x_*} \mathcal{M}$. They are therefore intrinsic and are called the symplectic eigenvalues of $\text{Hess}_{\mathcal{M}} \mathcal{E}(x_*)$.

Denoting by $Y(t) \in \mathbb{R}^{2n}$ the column vector containing the coefficients of $y(t)$ in the basis $(u_1, \dots, u_n, J_{x_*} u_1, \dots, J_{x_*} u_n)$ and by

$$Z(t) := \begin{pmatrix} \Omega^{-1/2} & 0 \\ 0 & \Omega^{1/2} \end{pmatrix} S^{-1} Y(t) =: \begin{pmatrix} q(t) \\ p(t) \end{pmatrix} \quad \text{with} \quad q(t), p(t) \in \mathbb{R}^n,$$

we have

$$\frac{dZ}{dt}(t) = J \nabla \mathfrak{H}_*^{\text{HO}}(Z(t)) \quad \text{with} \quad \mathfrak{H}_*^{\text{HO}}(Z) = \mathfrak{H}_*^{\text{HO}} \begin{pmatrix} q \\ p \end{pmatrix} = \frac{1}{2} |p|^2 + \frac{1}{2} q^T \Omega^2 q.$$

The angular frequencies $\omega_1, \dots, \omega_n$ therefore represent the excitation frequencies of the system in the linear response regime.

Let us finally consider the special case of separable Hamiltonians of the form

$$\mathfrak{H}_* = \begin{pmatrix} H^{\text{rr}} & 0 \\ 0 & H^{\text{ii}} \end{pmatrix} \in \mathbb{R}_{\text{sym}}^{2n \times 2n}. \quad (17)$$

Introducing the symplectic matrix

$$S = \begin{pmatrix} R & 0 \\ 0 & R^{-T} \end{pmatrix} \quad \text{with} \quad R = (H^{\text{rr}})^{-1/2} \left((H^{\text{rr}})^{1/2} H^{\text{ii}} (H^{\text{rr}})^{1/2} \right)^{1/4},$$

we get

$$S^T \mathfrak{H}_* S = \begin{pmatrix} \tilde{\Omega} & 0 \\ 0 & \tilde{\Omega} \end{pmatrix}, \quad \text{with} \quad \tilde{\Omega} = \left((H^{\text{rr}})^{1/2} H^{\text{ii}} (H^{\text{rr}})^{1/2} \right)^{1/2}. \quad (18)$$

Diagonalizing $\tilde{\Omega}$ readily provides the symplectic eigenvalues of \mathfrak{H}_* .

3 Dynamics on Grassmann manifolds (FCI, TDHF, TDDFT)

In this section, we restrict ourselves to the case when the Kähler manifold is the complex Grassmann manifold

$$\mathcal{M} = \text{Gr}_{\mathbb{C}}(r, n) = \{\gamma \in \mathbb{C}_{\text{herm}}^{n \times n} \mid \gamma^2 = \gamma, \text{Tr}(\gamma) = r\}, \quad (19)$$

where r, n are positive integers such that $1 \leq r \leq n-1$ (the trivial cases $\mathcal{M} = \text{Gr}_{\mathbb{C}}(0, n) = \{0\}$ and $\mathcal{M} = \text{Gr}_{\mathbb{C}}(n, n) = \{I_n\}$ are uninteresting). Such manifolds appear in quantum dynamics in at least two settings:

1. pure-state dynamics of generic isolated finite-dimensional quantum systems described by the linear Schrödinger equation, or equivalently the linear quantum Liouville equation (see Section 3.3). In computational quantum chemistry, this corresponds to the FCI level of theory;
2. mean-field models for many-body fermionic systems. This framework encompasses the cases of both TDHF and adiabatic TDDFT, for which the dynamics is governed by a system of coupled nonlinear Schrödinger equations, or equivalently a nonlinear quantum Liouville equation (see Section 3.4).

Before elaborating on these two fundamental examples, the geometry and Kähler structure of the complex Grassmann manifold $\text{Gr}_{\mathbb{C}}(r, n)$ are recalled in Sections 3.1 and 3.2, and the abstract Eqs. (8)-(10) are rewritten in a more concrete form in the special case when $\mathcal{M} = \text{Gr}_{\mathbb{C}}(r, n)$ in Sections 3.3 and 3.4. More details about Grassmann manifold can be found in the review articles in Refs.^{49,50} and the monographs in Refs.^{51,52}.

3.1 Geometry of complex Grassmann manifolds

The tangent space to the complex Grassmann manifold $\mathcal{M} = \text{Gr}_{\mathbb{C}}(r, n)$ at some $\gamma \in \mathcal{M}$ is given by

$$T_{\gamma}\mathcal{M} = \{Q \in \mathbb{C}_{\text{herm}}^{n \times n} \mid \gamma Q + Q\gamma = Q\}.$$

Any $\gamma \in \mathcal{M}$ can be decomposed as

$$\gamma = U \begin{pmatrix} I_r & 0 \\ 0 & 0 \end{pmatrix} U^*, \quad \text{with} \quad UU^* = U^*U = I_n,$$

and we then have

$$T_{\gamma}\mathcal{M} = \left\{ Q = U \begin{pmatrix} 0 & X \\ X^* & 0 \end{pmatrix} U^* \mid X \in \mathbb{C}^{r \times m} \right\} \quad \text{with} \quad m := n - r. \quad (20)$$

The Grassmann manifold \mathcal{M} can be endowed with the following Kähler structure:

- in view of Eq. (20), the tangent space $T_{\gamma}\mathcal{M}$ can be identified with the complex vector space $\mathbb{C}^{r \times m}$, endowed with the Hermitian inner product

$$\forall \gamma \in \mathcal{M}, \quad \forall Q_1, Q_2 \in T_{\gamma}\mathcal{M}, \quad \langle Q_1, Q_2 \rangle_{\gamma} := 2\text{Tr}(X_1^* X_2) = 2\text{Tr}(Q_1 \gamma Q_2 (1 - \gamma)),$$

where X_j is the matrix of $\mathbb{C}^{r \times m}$ such that

$$Q_j = U \begin{pmatrix} 0 & X_j \\ X_j^* & 0 \end{pmatrix} U^*, \quad j = 1, 2; \quad (21)$$

- Riemannian metric: using the properties

$$\gamma^2 = \gamma, \quad (1 - \gamma)^2 = 1 - \gamma, \quad \forall Q \in T_\gamma \mathcal{M}_\mathbb{R}, \quad \gamma Q + Q\gamma = Q \text{ i.e., } \gamma Q = Q(1 - \gamma), \quad (22)$$

we get, for any $\gamma \in \mathcal{M}_\mathbb{R}$ and $Q_1, Q_2 \in T_\gamma \mathcal{M}_\mathbb{R}$,

$$\begin{aligned} g_\gamma(Q_1, Q_2) &:= \text{Re}(\langle Q_1, Q_2 \rangle_\gamma) \\ &= \text{Tr}(X_1^* X_2) + \text{Tr}(X_1 X_2^*) \\ &= \text{Tr}(Q_1 \gamma Q_2 (1 - \gamma)) + \text{Tr}((1 - \gamma) Q_2 \gamma Q_1) \\ &= \text{Tr}(Q_1 \gamma Q_2) + \text{Tr}(Q_1 (1 - \gamma) Q_2) \\ &= \text{Tr}(Q_1 Q_2); \end{aligned}$$

- Symplectic form: we infer from Eq. (22) that, for any $\gamma \in \mathcal{M}_\mathbb{R}$ and $Q_1, Q_2 \in T_\gamma \mathcal{M}_\mathbb{R}$,

$$\begin{aligned} \omega_\gamma(Q_1, Q_2) &:= \text{Im}(\langle Q_1, Q_2 \rangle_\gamma) \\ &= -i \text{Tr}(Q_1 (2\gamma - 1) Q_2) \\ &= -i \text{Tr}(Q_2 (1 - 2\gamma) Q_1). \end{aligned}$$

Note that, still using Eq. (22), we have

$$\begin{aligned} \overline{\text{Tr}(Q_1 (2\gamma - 1) Q_2)} &= \text{Tr}(Q_2 (2\gamma - 1) Q_1) = 2 \text{Tr}(Q_2 \gamma Q_1) - \text{Tr}(Q_2 Q_1) \\ &= 2 \text{Tr}((1 - \gamma) Q_2 Q_1 (1 - \gamma)) - \text{Tr}(Q_2 Q_1) \\ &= \text{Tr}(Q_1 (1 - 2\gamma) Q_2) = -\text{Tr}(Q_1 (2\gamma - 1) Q_2), \end{aligned}$$

so that $\text{Tr}(Q_1 (2\gamma - 1) Q_2)$ is an imaginary number.

A simple calculation shows that the symplectic operator $J_\gamma : T_\gamma \mathcal{M}_\mathbb{R} \rightarrow T_\gamma \mathcal{M}_\mathbb{R}$ is given by

$$\forall Q \in T_\gamma \mathcal{M}_\mathbb{R}, \quad J_\gamma Q := -i[Q, \gamma]. \quad (23)$$

In the representation (21), it reads

$$\forall Q = U \begin{pmatrix} 0 & X \\ X^* & 0 \end{pmatrix} U^* \in T_\gamma \mathcal{M}_\mathbb{R}, \quad J_\gamma Q = U \begin{pmatrix} 0 & iX \\ -iX^* & 0 \end{pmatrix} U^*.$$

Recall that the orthogonal projector $P_\gamma : \mathbb{C}_{\text{herm}}^{n \times n} \rightarrow T_\gamma \mathcal{M}_\mathbb{R}$ (for the Frobenius inner product) has a simple expression:

$$\forall \gamma \in \mathcal{M}_\mathbb{R}, \quad \forall M \in \mathbb{C}_{\text{herm}}^{n \times n}, \quad P_\gamma M := \gamma M (1 - \gamma) + (1 - \gamma) M \gamma = [\gamma, [\gamma, M]], \quad (24)$$

and that in the representation (21),

$$\forall M = U \begin{pmatrix} A & B \\ B^* & C \end{pmatrix} U^* \in \mathbb{C}_{\text{herm}}^{n \times n}, \quad P_\gamma M = U \begin{pmatrix} 0 & B \\ B^* & 0 \end{pmatrix} U^*.$$

It follows by direct calculations that

$$\forall \gamma \in \mathcal{M}_\mathbb{R}, \quad \forall M \in \mathbb{C}_{\text{herm}}^{n \times n}, \quad i[\gamma, M] \in T_\gamma \mathcal{M}_\mathbb{R}, \quad [\gamma, [\gamma, [\gamma, M]]] = [\gamma, M]. \quad (25)$$

Finally, the exponential map is given by

$$\forall \gamma \in \mathcal{M}_\mathbb{R}, \quad \forall Q \in T_\gamma \mathcal{M}_\mathbb{R}, \quad \text{Exp}_\gamma(Q) = e^{[\gamma, Q]} \gamma e^{-[\gamma, Q]},$$

which in essence coincides with the exponential parametrization of molecular coefficients widely used in quantum chemistry⁵³.

3.2 Hamiltonian dynamics on Grassmann manifolds

Let $\mathcal{M} = \text{Gr}_{\mathbb{C}}(r, n)$ be a complex Grassmann manifold, $E : \mathbb{C}_{\text{herm}}^{n \times n} \rightarrow \mathbb{R}$ an energy functional, smooth in a neighborhood of $\mathcal{M}_{\mathbb{R}}$, and $\mathcal{E} : \mathcal{M}_{\mathbb{R}} \rightarrow \mathbb{R}$ the restriction of E to $\mathcal{M}_{\mathbb{R}}$. Denoting by $H_{\gamma} := \nabla E(\gamma) \in \mathbb{C}_{\text{herm}}^{n \times n}$ the gradient of E at $\gamma \in \mathcal{M}_{\mathbb{R}}$ (for the Frobenius inner product), we have

$$\text{grad}_{\mathcal{M}} \mathcal{E}(\gamma) = P_{\gamma}(\nabla E(\gamma)) = P_{\gamma}(H_{\gamma}) = [\gamma, [\gamma, H_{\gamma}]]. \quad (26)$$

Using Eqs. (23) and (25), we get

$$\forall \gamma \in \mathcal{M}_{\mathbb{R}}, \quad J_{\gamma} \text{grad}_{\mathcal{M}} \mathcal{E}(\gamma) = -i[\text{grad}_{\mathcal{M}} \mathcal{E}(\gamma), \gamma] = -i[[\gamma, [\gamma, H_{\gamma}]], \gamma] = -i[H_{\gamma}, \gamma].$$

The symplectic dynamics (8) generated by the energy functional \mathcal{E} is thus given by

$$\frac{d\gamma}{dt}(t) = -i[H_{\gamma(t)}, \gamma(t)] \quad (\text{Kähler dynamics on Grassmann manifolds}). \quad (27)$$

Stationary points γ_{\star} are characterized by the equation

$$[H_{\gamma_{\star}}, \gamma_{\star}] = 0 \quad (\text{critical points on Grassmann manifolds}). \quad (28)$$

This equilibrium condition implies that there exists a unitary matrix $U_{\star} \in U(n)$ such that

$$\gamma_{\star} = U_{\star} \begin{pmatrix} I_r & 0 \\ 0 & 0 \end{pmatrix} U_{\star}^* \quad \text{and} \quad H_{\gamma_{\star}} = U_{\star} \begin{pmatrix} E^r & 0 \\ 0 & E^m \end{pmatrix} U_{\star}^*, \quad (29)$$

where $E^r \in \mathbb{C}_{\text{herm}}^{r \times r}$ and $E^m \in \mathbb{C}_{\text{herm}}^{m \times m}$ are real diagonal matrices.

As \mathcal{M} is a Riemannian submanifold of $\mathbb{C}_{\text{herm}}^{n \times n}$, the Riemannian Hessian on \mathcal{E} is given by

$$\forall Q \in T_{\gamma_{\star}} \mathcal{M}_{\mathbb{R}}, \quad \text{Hess}_{\mathcal{M}} \mathcal{E}(\gamma_{\star})(Q) = P_{\gamma_{\star}}([D\mathcal{G}(\gamma_{\star})](Q)),$$

where $\mathcal{G} : \mathbb{C}_{\text{herm}}^{n \times n} \rightarrow \mathbb{C}_{\text{herm}}^{n \times n}$ is any smooth extension of $\text{grad}_{\mathcal{M}} \mathcal{E}(\gamma)$ in a neighborhood of $\mathcal{M}_{\mathbb{R}}$. In view of (26), an obvious extension is

$$\mathcal{G}(M) := [M, [M, \nabla E(M)]],$$

for which

$$\begin{aligned} [D\mathcal{G}(\gamma_{\star})](Q) &= \underbrace{[Q, [\gamma_{\star}, H_{\gamma_{\star}}]]}_{=0 \text{ by Eq. (28)}} + \underbrace{[\gamma_{\star}, [Q, H_{\gamma_{\star}}]]}_{\in T_{\gamma_{\star}} \mathcal{M}_{\mathbb{R}} \text{ if } Q \in T_{\gamma_{\star}} \mathcal{M}_{\mathbb{R}}} + \underbrace{[\gamma_{\star}, [\gamma_{\star}, D^2 E(\gamma_{\star})(Q)]]}_{=P_{\gamma_{\star}}(D^2 E(\gamma_{\star})(Q))} \end{aligned}$$

where $D^2 E(\gamma_{\star}) : \mathbb{C}_{\text{herm}}^{n \times n} \rightarrow \mathbb{C}_{\text{herm}}^{n \times n}$ is the second derivative of E at γ_{\star} . The Riemannian Hessian $\text{Hess}_{\mathcal{M}} \mathcal{E}(\gamma_{\star}) : T_{\gamma_{\star}} \mathcal{M}_{\mathbb{R}} \rightarrow T_{\gamma_{\star}} \mathcal{M}_{\mathbb{R}}$ is thus given by

$$\text{Hess}_{\mathcal{M}} \mathcal{E}(\gamma_{\star})(Q) = [\gamma_{\star}, [Q, H_{\gamma_{\star}}]] + P_{\gamma_{\star}}(D^2 E(\gamma_{\star})(Q)). \quad (30)$$

Using Eqs. (25) and (28), we finally obtain that the linearized dynamics is given by

$$\frac{dQ}{dt}(t) = -i[H_{\gamma_{\star}}, Q] - i[D^2 E(\gamma_{\star})Q, \gamma_{\star}] \quad (\text{linear response on Grassmann manifolds}) \quad (31)$$

where we used the fact that Eqs. (22) and (23) imply

$$\forall Q \in T_{\gamma_{\star}} \mathcal{M}_{\mathbb{R}}, \quad J_{\gamma_{\star}}([\gamma_{\star}, [Q, H_{\gamma_{\star}}]]) = -i[[\gamma_{\star}, [Q, H_{\gamma_{\star}}]], \gamma_{\star}] = -i[H_{\gamma_{\star}}, Q].$$

3.3 Linear energy functionals on projective spaces (FCI)

Consider an isolated quantum system with finite-dimensional state space \mathcal{H} . In the quantum chemistry applications we have in mind, \mathcal{H} is the FCI N -electron state-space generated by the N_b atomic spin-orbitals of the discretization basis, and is therefore of dimension $n = \binom{N_b}{N}$.

The space \mathcal{H} can be identified with \mathbb{C}^n by the choice of an orthonormal basis. The postulates of quantum mechanics imply that the set of FCI pure states of the system can be identified with the projective space $P(\mathcal{H}) \cong \mathbb{C}P^{n-1} \cong \text{Gr}(1, n)$. Recall that an element of $\mathbb{C}P^{n-1}$ can be represented by

1. a normalized vector $\psi \in \mathbb{C}^n$, it being understood that ψ and $e^{i\theta}\psi$, with any $\theta \in \mathbb{R}$, represent the same element of $\mathbb{C}P^{n-1}$. This representation is the usual one in quantum mechanics (wavefunction formalism);
2. a non-zero vector $\tilde{\psi} \in \mathbb{C}^n$, it being understood that $\tilde{\psi}$ and $\lambda\tilde{\psi}$, with any $\lambda \in \mathbb{C} \setminus \{0\}$, represent the same element of $\mathbb{C}P^{n-1}$;
3. a unique element $\Gamma \in \text{Gr}_{\mathbb{C}}(1, n)$. This representation is used in the density-matrix formulation of quantum mechanics.

The connection between these three representations is

$$\Gamma = \psi\psi^* = \frac{\tilde{\psi}\tilde{\psi}^*}{|\tilde{\psi}|^2} \quad \text{or, using Dirac's bra-ket notation,} \quad \Gamma = |\psi\rangle\langle\psi| = \frac{|\tilde{\psi}\rangle\langle\tilde{\psi}|}{\langle\tilde{\psi}|\tilde{\psi}\rangle}.$$

Let $H \in \mathbb{C}_{\text{herm}}^{n \times n}$ be the Hamiltonian matrix of the system in the chosen orthonormal basis of the FCI N -electron state-space. Let $E : \mathbb{C}_{\text{herm}}^{n \times n} \rightarrow \mathbb{R}$ be the linear energy functional defined by $E(\Gamma) = \text{Tr}(H\Gamma)$. The FCI energy functional is the restriction \mathcal{E} of E to $\text{Gr}_{\mathbb{C}}(1, n)$:

$$\mathcal{E}(\Gamma) = \text{Tr}(H\Gamma) = \langle\psi|H|\psi\rangle = \frac{\langle\tilde{\psi}|H|\tilde{\psi}\rangle}{\langle\tilde{\psi}|\tilde{\psi}\rangle}.$$

The FCI approximation is thus a special case of the general framework described in Section 3.2, corresponding to $r = 1$, $n = \binom{N_b}{N}$, and $E : \mathbb{C}_{\text{herm}}^{n \times n} \rightarrow \mathbb{R}$ linear. The dynamics (27) then reads

$$\frac{d\Gamma}{dt}(t) = -i[H, \Gamma(t)], \quad i\frac{d\psi}{dt}(t) = H\psi(t) - \beta(t)\psi(t), \quad i\frac{d\tilde{\psi}}{dt}(t) = H\tilde{\psi}(t) - \mu(t)\tilde{\psi}(t), \quad (32)$$

where $\beta(t) \in \mathbb{R}$, $\mu(t) \in \mathbb{C}$ are gauge parameters. Steady states (see Eq. (28)) are characterized by

$$[H, \Gamma_{\star}] = 0, \quad \left\{ \begin{array}{l} H\psi_{\star} = E\psi_{\star}, \\ \|\psi_{\star}\| = 1, \\ \psi_{\theta}(t) = e^{i\theta(t)}\psi_{\star}, \end{array} \right. , \quad \left\{ \begin{array}{l} H\tilde{\psi}_{\star} = E\tilde{\psi}_{\star}, \\ \tilde{\psi}_{\lambda}(t) = e^{\lambda(t)}\tilde{\psi}_{\star}. \end{array} \right.$$

In particular, the local minimizers of \mathcal{E} are global and are the ground-states of H and the assumption that the ground-state Γ_{\star} is nondegenerate is equivalent to the assumption that the ground-state eigenvalue E_0 of H is simple. Other critical points of \mathcal{E} are then exactly the excited states of H , corresponding to the energies $E_1 \leq E_2 \leq \dots \leq E_{n-1}$, and the excitation energies determined by CP are $\omega_k^{\text{CP-FCI}} = E_k - E_0$ ($k = 1, \dots, n-1$).

Let us turn to LR. Due to the fact that the energy functional $E(\Gamma) = \text{Tr}(H\Gamma)$ is linear in Γ , we have $H_{\Gamma_\star} = \nabla E(\Gamma_\star) = H$ and $D^2E(\Gamma_\star) = 0$. It follows that the linear response Eq. (31) around a steady state $\Gamma_\star = |\Psi_\star\rangle\langle\Psi_\star|$ on $\text{Gr}_{\mathbb{C}}(1, n)$ (with $H\Psi_\star = E_0\Psi_\star$) reads

$$\frac{dQ}{dt}(t) = -i[H, Q(t)] \quad \text{on} \quad T_{\Gamma_\star}\text{Gr}_{\mathbb{C}}(1, n)_{\mathbb{R}}. \quad (33)$$

Using an orthonormal basis of the FCI Hamiltonian, in which the first basis vector is Ψ_\star , to identify the discretized N -particle state space with \mathbb{C}^n , $n = \binom{N_b}{N}$, the representation in Eq. (29) for $r = 1$ can be rewritten as

$$\begin{aligned} \Gamma_\star &= \begin{pmatrix} 1 & 0 \\ 0 & 0 \end{pmatrix}, \quad Q = \begin{pmatrix} 0 & \Psi^* \\ \Psi & 0 \end{pmatrix}, \quad \Psi \in \mathbb{C}^{n-1}, \\ -i[H, Q] &= \begin{pmatrix} 0 & ((H|_{\Psi_\star^\perp} - E_0)\Psi)^* \\ (H|_{\Psi_\star^\perp} - E_0)\Psi & 0 \end{pmatrix}, \end{aligned}$$

where $H|_{\Psi_\star^\perp} \in \mathbb{C}_{\text{herm}}^{(n-1) \times (n-1)}$ denotes the projection of H onto Ψ_\star^\perp . Consequently, Eq. (33) is equivalent to

$$i\frac{d\Psi}{dt}(t) = (H|_{\Psi_\star^\perp} - E_0)\Psi(t) \quad \text{on} \quad \Psi_\star^\perp,$$

which shows that the LR-FCI excitation energies are given as expected by $\omega_k^{\text{LR-FCI}} = E_k - E_0$ ($k = 1, \dots, n-1$).

In summary, we recover the well-known fact that both CP and LR are exact for linear quantum Hamiltonians (FCI level of theory in quantum chemistry).

3.4 Mean-field models (TDHF and adiabatic TDDFT)

Let us now consider the case of mean-field models. We will focus on general HF (GHF) models, in which non-collinear spin states are allowed. However, the formalism presented here can be easily adapted to restricted and unrestricted HF models, more widely used in applications, as well as restricted/unrestricted adiabatic TDDFT.

We still denote by N_b the number of atomic spin-orbitals of the chosen discretization basis, and assume that these functions are real-valued, which is the case for standard atomic orbital basis sets. We also assume that the system is not subjected to an external magnetic field and that spin-orbit coupling terms are neglected. In this case, it makes sense to seek HF or Kohn-Sham ground states satisfying time-reversal symmetry, leading to real-valued HF or Kohn-Sham occupied orbitals, and real-symmetric Fock or Kohn-Sham matrices at the ground state. In the rest of the section, we work in an orthonormal basis of the one-particle state-space \mathcal{H} consisting of N_b real occupied/virtual molecular spin-orbitals $(\varphi_1, \dots, \varphi_{N_b})$ at the GHF ground state γ_\star with energies ranked in nondecreasing order. We denote by $h \in \mathbb{C}_{\text{herm}}^{N_b \times N_b}$ the one-electron Hamiltonian matrix with

$$h_{pq} := \int_{\mathbb{R}^3 \times \{\alpha, \beta\}} \varphi_p(\mathbf{x}) \widehat{h} \varphi_q(\mathbf{x}) \, d\mathbf{x}, \quad \text{where } \widehat{h} \text{ is the one-body Hamiltonian,}$$

and by

$$(pq|rs) := \int_{\mathbb{R}^3 \times \{\alpha, \beta\}} \int_{\mathbb{R}^3 \times \{\alpha, \beta\}} \frac{\overline{\varphi_p(\mathbf{x})} \varphi_q(\mathbf{x}) \overline{\varphi_r(\mathbf{x}')} \varphi_s(\mathbf{x}')}{|\mathbf{r} - \mathbf{r}'|} \, d\mathbf{x} \, d\mathbf{x}'$$

the two-electron integrals in this basis. Here, $\mathbf{x} = (\mathbf{r}, \sigma)$ denotes the spatial and spin coordinates. Note that for the chosen basis, the complex conjugation in the above formula can be omitted as the basis functions are real. We also use the standard notation

$$(pq||rs) := (pq|rs) - (ps|rq).$$

The GHF energy functional E^{GHF} is given by

$$E^{\text{GHF}}(\gamma) = \text{Tr}(h\gamma) + \frac{1}{2}\text{Tr}(G(\gamma)\gamma),$$

where $G : \mathbb{C}_{\text{herm}}^{N_b \times N_b} \rightarrow \mathbb{C}_{\text{herm}}^{N_b \times N_b}$ is defined as $G(\gamma) = J(\gamma) - K(\gamma)$, with $J, K : \mathbb{C}_{\text{herm}}^{N_b \times N_b} \rightarrow \mathbb{C}_{\text{herm}}^{N_b \times N_b}$ the Coulomb and exchange functionals, respectively:

$$[J(\gamma)]_{pq} := \sum_{r,s=1}^{N_b} (pq|rs)\gamma_{sr}, \quad [K(\gamma)]_{pq} := \sum_{\mu,\nu=1}^{N_b} (ps|rq)\gamma_{sr}. \quad (34)$$

It follows that $H_\gamma := \nabla E^{\text{GHF}}(\gamma) = h + G(\gamma)$ is the Fock matrix, that (27) coincides with the usual TDHF equations, and (28) with the McWeeny formulation of the HF equations. In GHF theory, the no-unfilled shell property proved in Ref.⁵⁴ in the continuous setting also holds in the discretized setting. We therefore have that in the chosen basis of occupied/virtual real molecular spin-orbitals

$$\gamma_\star = \begin{pmatrix} I_N & 0 \\ 0 & 0 \end{pmatrix}, \quad H_{\gamma_\star} = \begin{pmatrix} \text{diag}(\varepsilon_1, \dots, \varepsilon_N) & 0 \\ 0 & \text{diag}(\varepsilon_{N+1}, \dots, \varepsilon_{N_b}) \end{pmatrix}, \quad (35)$$

$$\text{with } \varepsilon_1 \leq \dots \leq \varepsilon_N < \varepsilon_{N+1} \leq \dots \leq \varepsilon_{N_b}. \quad (36)$$

Let us now show that the Kähler formalism provide a simple alternative to Casida's derivation of LR excitation energies for mean-field models. Following the systematic strategy described in Section 2, it indeed suffices to select a basis

$$(u_1, \dots, u_{N(N_b-N)}, J_{\gamma_\star} u_1, \dots, J_{\gamma_\star} u_{N(N_b-N)})$$

of $T_{\gamma_\star} \mathcal{M}_{\mathbb{R}}$, build the matrix \mathfrak{H}_\star defined in Eq. (11) with entries given by Eqs. (12)-(15), and compute the symplectic eigenvalues of \mathfrak{H}_\star . Choosing the canonical basis of $T_{\gamma_\star} \mathcal{M}_{\mathbb{R}}$, that is

$$u_{[ia]} := \frac{1}{\sqrt{2}} \begin{pmatrix} 0 & e_{[ia]} \\ e_{[ia]}^T & 0 \end{pmatrix}, \quad J_{\gamma_\star} u_{[ia]} = \frac{1}{\sqrt{2}} \begin{pmatrix} 0 & ie_{[ia]} \\ -ie_{[ia]}^T & 0 \end{pmatrix}, \quad \text{with } [e_{[ia]}]_{jb} = \delta_{(ia),(jb)},$$

for $1 \leq i \leq N$ and $N+1 \leq j \leq N_b$, we deduce from Eq. (30), the fact that $D^2 E^{\text{GHF}}(\gamma)(Q) = G(Q)$, and the real character of the spin-orbitals that

$$\mathfrak{H}_\star^{\text{GHF}} = \begin{pmatrix} A + B & 0 \\ 0 & A - B \end{pmatrix}, \quad (37)$$

where the entries of the matrices A and B are given respectively by

$$A_{ai,bj} := (\varepsilon_a - \varepsilon_i)\delta_{ij}\delta_{ab} + (ai||jb), \quad B_{ai,bj} := (ai||bj).$$

These matrices are the GHF analogues of the A and B matrices in LR-TDDFT Casida's equations. The linearized dynamics Hamiltonian is therefore separable and the matrix $\tilde{\Omega}$ in Eq. (18) then reads in this specific case

$$\tilde{\Omega} = \left((A + B)^{1/2} (A - B) (A + B)^{1/2} \right)^{1/2},$$

an expression in agreement with Ref.⁵⁵ Eqs. (II.78)-(II.79).

4 Theoretical analysis in the weakly-interacting regime

In this part, we aim to compare theoretically, in the weakly-interacting regime, the CP and LR formalisms for computing the electronic excitation energies at the FCI and HF levels of theory. We consider a family of Hamiltonians parametrized by an additional coupling parameter λ that modulates the degree of interaction within the energy functional. In the non-interacting limit ($\lambda = 0$), HF and FCI lead to the same ground and excited state energies, so that CP-HF provides the same sequence of excitation energies as FCI, while LR-HF returns the subsequence of excitation energies corresponding to single excitations. Under a nondegeneracy assumption, we are able to compute the FCI (Section 4.1), as well as CP-HF and LR-HF (Section 4.2) excitation energies up to second-order errors in λ in the weakly-interacting regime ($|\lambda| \ll 1$). To our knowledge, this is the first study aiming at comparing the CP and LR methodologies from a theoretical point of view. These theoretical findings are substantiated by numerical results in Section 5. We shall remark that although the cases of $\lambda \neq 1$ are non-physical, our analysis could offer potential insights into the study of more complicated real molecules.

In this section, we consider a system with $N = 2N_p$ electrons (N_p is the number of electron pairs) in N_b atomic orbitals (hence $2N_b$ atomic spin-orbitals) and the family of second-quantized Hamiltonians on the Fock space $\text{Fock}(\mathbb{C}^{2N_b})$ defined by

$$\hat{H}_\lambda := \hat{h} + \lambda \hat{V} = \sum_{\kappa, \lambda=1}^{N_b} h_{\kappa\lambda} \sum_{\sigma \in \{\alpha, \beta\}} \hat{a}_{\kappa\sigma}^\dagger \hat{a}_{\lambda\sigma} + \frac{\lambda}{2} \sum_{\kappa, \lambda, \mu, \nu=1}^{N_b} \sum_{\sigma, \sigma' \in \{\alpha, \beta\}} (\kappa\sigma, \mu\sigma | \lambda\sigma', \nu\sigma') \hat{a}_{\kappa\sigma}^\dagger \hat{a}_{\lambda\sigma'}^\dagger \hat{a}_{\nu\sigma'} \hat{a}_{\mu\sigma},$$

where $\lambda \geq 0$ is a coupling parameter. Let $(\phi_n^0)_{1 \leq n \leq N_b}$ be an orthonormal basis of \mathbb{C}^{N_b} diagonalizing the one-electron Hermitian matrix h , such that

$$h\phi_n^0 = \varepsilon_n^0 \phi_n^0 \quad \text{with} \quad \varepsilon_1^0 \leq \dots \leq \varepsilon_{N_b}^0.$$

To avoid technicalities, we assume that

(H) the eigenvalues of h are nondegenerate and the $\binom{N_b}{N_p}$ real numbers obtained by summing up N_p of the N_b eigenvalues of h are all different.

4.1 Analysis at the FCI level of theory

It follows from Assumption (H) that the only degeneracies in the eigenstates of \hat{H}_0 in the N -particle sector are due to degenerate spin states. Restricting our analysis to the $S_z = 0$ spin sector, each state has N_p spin-up electrons and N_p spin-down electrons, the N -electron ground state of \hat{H}_0 is a nondegenerate singlet state given by

$$\Phi_0^{(0)} := \frac{1}{\sqrt{N!}} (\phi_1^0 \otimes \alpha) \wedge (\phi_1^0 \otimes \beta) \wedge \dots \wedge (\phi_{N_p}^0 \otimes \alpha) \wedge (\phi_{N_p}^0 \otimes \beta),$$

and the first excited state is two-fold degenerate, spanned by

$$\begin{aligned} \Phi_\alpha^{(0)} &:= \frac{1}{\sqrt{N!}} (\phi_1^0 \otimes \alpha) \wedge (\phi_1^0 \otimes \beta) \wedge \dots \wedge (\phi_{N_p-1}^0 \otimes \alpha) \wedge (\phi_{N_p-1}^0 \otimes \beta) \wedge (\phi_{N_p+1}^0 \otimes \alpha) \wedge (\phi_{N_p}^0 \otimes \beta), \\ \Phi_\beta^{(0)} &:= \frac{1}{\sqrt{N!}} (\phi_1^0 \otimes \alpha) \wedge (\phi_1^0 \otimes \beta) \wedge \dots \wedge (\phi_{N_p-1}^0 \otimes \alpha) \wedge (\phi_{N_p-1}^0 \otimes \beta) \wedge (\phi_{N_p}^0 \otimes \alpha) \wedge (\phi_{N_p+1}^0 \otimes \beta). \end{aligned}$$

Note that $\Phi_\alpha^{(0)}$ and $\Phi_\beta^{(0)}$ are not eigenfunctions of \mathbf{S}^2 , but that $\Psi_S^{(0)} := (\Phi_\alpha^{(0)} - \Phi_\beta^{(0)})/\sqrt{2}$ is a singlet state (the first-excited state in the $\mathbf{S}^2 = 0$ sector) and $\Psi_T^{(0)} := (\Phi_\alpha^{(0)} + \Phi_\beta^{(0)})/\sqrt{2}$ the

$S_z = 0$ component of a triplet state (the ground state in the $\mathbf{S}^2 = 2$ sector). The energies of the ground state $\Phi_0^{(0)}$ and the two-fold degenerate first excited state are respectively

$$E_0^{(0)} = 2 \sum_{i=1}^{N_p} \varepsilon_i^0 \quad \text{and} \quad E_\alpha^{(0)} = E_\beta^{(0)} = E_S^{(0)} = E_T^{(0)} = E_0^{(0)} + \varepsilon_{N_p+1} - \varepsilon_{N_p}.$$

It follows from standard nondegenerate perturbation theory that for small λ , the ground state of \widehat{H}_λ is nondegenerate and its energy $E_0(\lambda)$ is a real-analytic function of λ . Likewise the first excited state in the $\mathbf{S}^2 = 0$ sector as well as the ground state in the $\mathbf{S}^2 = 2$ sector are nondegenerate, and their energies $E_S(\lambda)$ and $E_T(\lambda)$ are real-analytic functions of λ for $|\lambda| \ll 1$. Consequently, so are the FCI excitation energies $\omega_S^{\text{FCI}}(\lambda) := E_S(\lambda) - E_0(\lambda)$ and $\omega_T^{\text{FCI}}(\lambda) := E_T(\lambda) - E_0(\lambda)$:

$$\omega_S^{\text{FCI}}(\lambda) = \sum_{k=0}^{+\infty} \lambda^k \omega_S^{\text{FCI},(k)}, \quad \omega_T^{\text{FCI}}(\lambda) = \sum_{k=0}^{+\infty} \lambda^k \omega_T^{\text{FCI},(k)},$$

where

$$\omega_S^{\text{FCI},(0)} = \omega_T^{\text{FCI},(0)} = \omega_{\text{HOMO-LUMO}}^{(0)} := \varepsilon_{N_p+1} - \varepsilon_{N_p}.$$

The coefficients $\omega_S^{(1)}$ and $\omega_T^{(1)}$ can be easily obtained by first-order perturbation theory:

$$\begin{aligned} \omega_{S/T}^{\text{FCI},(1)} &= \sum_{j=1}^{N_p-1} ((N_p+1)\beta, (N_p+1)\beta || j\beta, j\beta) - \sum_{j=1}^{N_p-1} (N_p\beta, N_p\beta || j\beta, j\beta) \\ &\quad + \sum_{j=1}^{N_p} ((N_p+1)\beta, (N_p+1)\beta || j\alpha, j\alpha) - \sum_{j=1}^{N_p} (N_p\beta, N_p\beta || j\alpha, j\alpha) \\ &\quad \pm (N_p\beta, (N_p+1)\beta || (N_p+1)\alpha, N_p\alpha). \end{aligned} \quad (38)$$

4.2 Analysis at the UHF level of theory

Let us now consider the UHF approximation, for which the underlying manifold is $\mathcal{M} = \text{Gr}_{\mathbb{C}}(N_p, N_b) \times \text{Gr}_{\mathbb{C}}(N_p, N_b)$. The UHF approximation of \widehat{H}_λ gives rise to a parametrized family of energy functionals of the form

$$\begin{aligned} E^{\text{UHF}}(\lambda, \gamma_\alpha, \gamma_\beta) &= \text{Tr}(h\gamma_\alpha) + \text{Tr}(h\gamma_\beta) + \frac{\lambda}{2} \text{Tr}(J(\gamma_\alpha + \gamma_\beta)(\gamma_\alpha + \gamma_\beta)) \\ &\quad - \frac{\lambda}{2} \text{Tr}(K(\gamma_\alpha)\gamma_\alpha) - \frac{\lambda}{2} \text{Tr}(K(\gamma_\beta)\gamma_\beta), \end{aligned} \quad (39)$$

where J and K are defined in Eq. (34).

CP-UHF. The critical points of $\mathcal{M} \ni (\gamma_\alpha, \gamma_\beta) \mapsto \mathcal{E}^{\text{UHF}}(0, \gamma_\alpha, \gamma_\beta) = \text{Tr}(h\gamma_\alpha) + \text{Tr}(h\gamma_\beta) \in \mathbb{R}$ are the $(\gamma_{\alpha^*}, \gamma_{\beta^*}) \in \mathcal{M}$ satisfying $[h, \gamma_{\alpha^*}] = [h, \gamma_{\beta^*}] = 0$. Under the nondegeneracy assumption (H), these critical points are isolated and there are exactly $\binom{N_b}{N_p} \times \binom{N_b}{N_p}$ of them. The ground state is

$$\left(\gamma_{[\emptyset, \emptyset]}^{(0)}, \gamma_{[\emptyset, \emptyset]}^{(0)} \right) \quad \text{with} \quad \gamma_{[\emptyset, \emptyset]}^{(0)} = \sum_{j=1}^{N_p} \phi_j^0 \phi_j^{0T}, \quad (40)$$

and the excited states are

$$\left(\gamma_{\alpha, [I_\alpha, A_\alpha]}^{(0)}, \gamma_{\beta, [I_\beta, A_\beta]}^{(0)} \right) \quad \text{where} \quad \gamma_{\sigma, [I_\sigma, A_\sigma]} := \gamma_{[\emptyset, \emptyset]}^0 - \sum_{i \in I_\sigma} \phi_i^0 \phi_i^{0T} + \sum_{a \in A_\sigma} \phi_a^0 \phi_a^{0T}, \quad (41)$$

for $I_\sigma \subset \{1, \dots, N_p\}$, $A_\sigma \subset \{N_p + 1, \dots, N_b\}$, $|I| = |A| \geq 1$. It follows from a simple application of the analytic implicit function theorem that under the nondegeneracy assumption (H), there exist $\lambda_c > 0$ and $\binom{N_b}{N_p} \times \binom{N_b}{N_p}$ real-analytic functions

$$\left(\gamma_{\alpha, [I_\alpha, A_\alpha]}(\bullet), \gamma_{\beta, [I_\beta, A_\beta]}(\bullet) \right) : (-\lambda_c, \lambda_c) \rightarrow \mathcal{M},$$

$I_\alpha, I_\beta \subset \{1, \dots, N_p\}$, $A_\alpha, A_\beta \subset \{N_p + 1, \dots, N_b\}$, $|I_\alpha| = |A_\alpha|$, $|I_\beta| = |A_\beta|$, such that for any $\lambda \in (-\lambda_c, \lambda_c)$, the function $\mathcal{M} \ni (\gamma_\alpha, \gamma_\beta) \mapsto \mathcal{E}(\lambda, \gamma_\alpha, \gamma_\beta) \in \mathbb{R}$ has exactly $\binom{N_b}{N_p} \times \binom{N_b}{N_p}$ critical points, all isolated, nondegenerate, and given by $(\gamma_{\alpha, [I_\alpha, A_\alpha]}(\lambda), \gamma_{\beta, [I_\beta, A_\beta]}(\lambda))$. Note that, by symmetry, $\gamma_{\alpha, [\emptyset, \emptyset]}(\lambda) = \gamma_{\beta, [\emptyset, \emptyset]}(\lambda) =: \gamma_{[\emptyset, \emptyset]}(\lambda)$, i.e., the UHF ground state coincides with the RHF ground state.

For $\lambda \in (-\lambda_c, \lambda_c)$, the excitation energies obtained by CP-UHF are thus the $\binom{N_b}{N_p} \times \binom{N_b}{N_p} - 1$ positive numbers

$$\omega_{[I_\alpha, A_\alpha], [I_\beta, A_\beta]}^{\text{CP-UHF}}(\lambda) := E^{\text{UHF}}(\lambda, \gamma_{\alpha, [I_\alpha, A_\alpha]}(\lambda), \gamma_{\beta, [I_\beta, A_\beta]}(\lambda)) - E^{\text{UHF}}(\lambda, \gamma_{[\emptyset, \emptyset]}(\lambda), \gamma_{[\emptyset, \emptyset]}(\lambda)) \quad (42)$$

with $I_\sigma \subset \{1, \dots, N_p\}$, $A_\sigma \subset \{N_p + 1, \dots, N_b\}$, $|I_\sigma| = |A_\sigma|$, $|I_\alpha| + |I_\beta| = |A_\alpha| + |A_\beta| \geq 1$. In addition, the functions $\omega_{[I_\alpha, A_\alpha], [I_\beta, A_\beta]}^{\text{CP-UHF}} : (-\lambda_c, \lambda_c) \rightarrow \mathbb{R}$ are real-analytic and it holds

$$\omega_{[I_\alpha, A_\alpha], [I_\beta, A_\beta]}^{\text{CP-UHF}}(\lambda) = \sum_{k=0}^{+\infty} \lambda^k \omega_{[I_\alpha, A_\alpha], [I_\beta, A_\beta]}^{\text{CP-UHF}, (k)}$$

with

$$\begin{aligned} \omega_{[I_\alpha, A_\alpha], [I_\beta, A_\beta]}^{\text{CP-UHF}, (0)} &= \sum_{a \in A_\alpha \cup A_\beta} \varepsilon_a^0 - \sum_{i \in I_\alpha \cup I_\beta} \varepsilon_i^0, \\ \omega_{[I_\alpha, A_\alpha], [I_\beta, A_\beta]}^{\text{CP-UHF}, (1)} &= \frac{\partial E^{\text{UHF}}}{\partial \lambda} \left(0, \gamma_{\alpha, [I_\alpha, A_\alpha]}^{(0)}, \gamma_{\beta, [I_\beta, A_\beta]}^{(0)} \right) - \frac{\partial E^{\text{UHF}}}{\partial \lambda} \left(0, \gamma_{[\emptyset, \emptyset]}^{(0)}, \gamma_{[\emptyset, \emptyset]}^{(0)} \right). \end{aligned}$$

The first-order variation of the excitation energy for the first excited state, given by the HOMO-LUMO excitation is

$$\begin{aligned} \omega_{\text{HOMO-LUMO}}^{\text{CP-UHF}, (1)} &:= \omega_{[\emptyset, \emptyset], [N_p, N_p+1]}^{\text{CP-UHF}, (1)} = \omega_{[N_p, N_p+1], [\emptyset, \emptyset]}^{\text{CP-UHF}, (1)} \\ &= \sum_{i=1}^{N_p-1} ((N_p + 1)\sigma, (N_p + 1)\sigma || i\sigma, i\sigma) + \sum_{i=1}^{N_p} ((N_p + 1)\beta, (N_p + 1)\beta | i\alpha, i\alpha) \\ &\quad - \sum_{i=1}^{N_p-1} (N_p\sigma, N_p\sigma || i\sigma, i\sigma) - \sum_{i=1}^{N_p} (N_p\beta, N_p\beta | i\alpha, i\alpha) \end{aligned} \quad (43)$$

for $\sigma = \alpha$ or β .

LR-UHF. Let us now turn to the LR-UHF approximation of excitation energies. First, as the complex dimension of the manifold \mathcal{M} is $2N_p(N_b - N_p)$, there are at most $2N_p(N_b - N_p)$ of them. For $\lambda = 0$, they can be interpreted as single excitations:

$$\omega_{[i, a]}^{\text{LR-UHF}, (0)} := \omega_{[i, a], [\emptyset, \emptyset]}^{\text{LR-UHF}, (0)} = \omega_{[\emptyset, \emptyset], [i, a]}^{\text{LR-UHF}, (0)} = \varepsilon_a^0 - \varepsilon_i^0, \quad 1 \leq i \leq N_p, \quad N_p + 1 \leq a \leq N_b.$$

Using again the analytic implicit functional theorem, it can be shown that for λ small enough, the excitation energies computed by linear response are given by real-analytic functions $(-\lambda_c, \lambda_c) \ni \lambda \mapsto \omega_{[i,a]}^{\text{LR-UHF}}(\lambda) \in \mathbb{R}$ such that $\omega_{[i,a]}^{\text{LR-UHF}}(0) = \omega_{[i,a]}^{\text{LR-UHF},(0)}$. In particular, the first excited state corresponds to the HOMO-LUMO transition and the first-order variation is given by

$$\begin{aligned}
\omega_{\text{HOMO-LUMO}}^{\text{LR-UHF},(1)} &:= \omega_{[N_p, N_p+1]}^{\text{LR-UHF},(1)} \\
&= \sum_{j=1}^{N_p-1} ((N_p+1)\beta, (N_p+1)\beta || j\beta, j\beta) - \sum_{j=1}^{N_p-1} (N_p\beta, N_p\beta || j\beta, j\beta) \\
&\quad + \sum_{j=1}^{N_p} ((N_p+1)\beta, (N_p+1)\beta | j\alpha, j\alpha) - \sum_{j=1}^{N_p} (N_p\beta, N_p\beta | j\alpha, j\alpha) \\
&\quad - (N_p\beta, (N_p+1)\beta | (N_p+1)\alpha, N_p\alpha). \tag{44}
\end{aligned}$$

Notice that this expression coincides with the one found in the FCI case, in Eq. (38). Therefore, in the non-interacting limit, FCI and UHF-LR are equivalent in computing single excitation energies, while they differ in the interacting case.

5 Numerical simulations

We perform proof-of-concept numerical simulations to support our theoretical findings. In Section 5.1, we compare the CP and LR formalisms in UHF theory for the H_2 , H_4 , and H_2O molecules, with a varying coupling parameter λ . The exact FCI theory is taken as reference. In particular, we check the analytical first-order derivatives of the excitation energies at $\lambda = 0$ given by Eqs. (43) and (44) vs the numerical ones obtained by local linear fits. In Section 5.2, we demonstrate that multiple critical points can arise even for the H_4 molecule (rectangular geometry) at the UHF/STO-3G level of theory. The energies of the critical points and their overlaps with the exact FCI excited states are shown as functions of λ . We note that in this section, only the index-1 saddle points (namely, the critical points where the Riemannian Hessian has exactly one negative eigenvalue) are considered in the CP formalism and they are computed numerically by using a constrained gentlest ascent dynamics, which is described in detail in another ongoing work. The approximate excitation energies in the LR formalism are found by solving Casida's equations²³⁻²⁵ using the open-source package PySCF⁵⁶.

5.1 Comparison of CP and LR formalisms within the UHF theory

In this Section, numerical experiments performed in the UHF framework are shown. Calculations have been performed with the minimal basis set STO-3G⁵⁷ and with the 3-21G basis⁵⁸, for the systems H_2 , H_4 in a linear and a rectangular geometry, and H_2O , with λ in the range $[0, 1]$. For H_2 , a bond length of 1 a.u. was considered; for the H_4 molecule, the linear geometry considers a bond length of 0.875 Å (Ref.⁵⁹); for the rectangular geometry, sides of 1 Å and 2 Å are considered. For the water molecule, the coordinates [O (0.00000000 0.00000000 0.11993333) a.u.], [H (0.00000000 -1.43497461 -0.95171452) a.u.], [H (0.00000000 1.43497461 -0.95171452) a.u.] were taken. We compare the first-order excitation energies of the HOMO-LUMO transition, obtained both with the LR and CP approaches. We note that for the CP results in this subsection, only the lowest excited states at $\lambda = 0$, which correspond to the HOMO-LUMO excitations, have been tracked

Table 1: First-order excitation energies for the HOMO-LUMO excitations of the molecules H_2 , H_4 in linear and rectangular geometry, and H_2O , obtained in the non-interacting regime of $\lambda \rightarrow 0$. For both CP and LR, the results obtained by the analytic expressions Eqs. (43) and (44), denoted here by $\omega_{\text{anal}}^{\text{CP,(1)}}$ and $\omega_{\text{anal}}^{\text{LR,(1)}}$, and numerically using a five-point scheme linear fit, denoted here by $\omega_{\text{num}}^{\text{CP,(1)}}$ and $\omega_{\text{num}}^{\text{LR,(1)}}$, are listed. The difference $\Delta\omega_{\text{anal}}^{(1)} = \omega_{\text{anal}}^{\text{CP,(1)}} - \omega_{\text{anal}}^{\text{LR,(1)}}$ between the two approaches is also shown.

Molecule (Basis)	$\omega_{\text{num}}^{\text{CP,(1)}}$	$\omega_{\text{anal}}^{\text{CP,(1)}}$	$\omega_{\text{num}}^{\text{LR,(1)}}$	$\omega_{\text{anal}}^{\text{LR,(1)}}$	$\Delta\omega_{\text{anal}}^{(1)}$
H_2 (STO-3G)	-0.012580	-0.012586	-0.182839	-0.182827	0.170241
H_2 (3-21G)	-0.330913	-0.330929	-0.422845	-0.422889	0.091960
H_4 lin. (STO-3G)	-0.107158	-0.107347	-0.245692	-0.245812	0.138465
H_4 lin. (3-21G)	-0.207375	-0.207529	-0.332364	-0.332485	0.124956
H_4 rect. (STO-3G)	0.052118	0.052118	-0.040455	-0.040246	0.092364
H_4 rect.(3-21G)	-0.061798	-0.061775	-0.133340	-0.133204	0.071429
H_2O (STO-3G)	-3.494042	-3.494149	-3.497100	-3.497208	0.003059

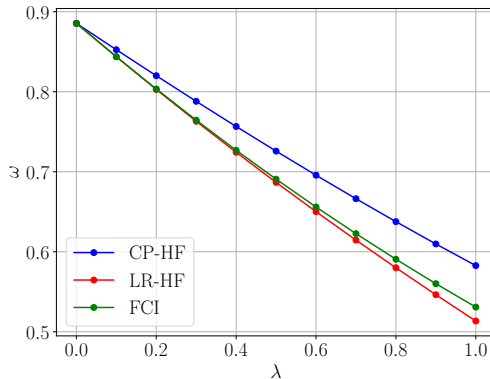


Figure 2: Dependence on the λ -parameter of the excitation energy, calculated on the H_2 molecule, with the 3-21G basis set.

across the range of λ . When λ increases, multiple critical points (with the same index) may emerge; see the discussions in Section 5.2.

The results displayed in Table 1 show for all examples a good agreement between the analytical derivatives obtained in Section 4 and linear fits of these quantities using the five points $(j \cdot \delta\lambda)_{0 \leq j \leq 4}$, with $\delta\lambda = 10^{-4}$ chosen small enough to be compatible with the limit $\lambda \rightarrow 0$, but not too small to avoid numerical instabilities. Furthermore, we can observe that, for the examples considered here, the difference calculated as $\omega_{\text{anal}}^{\text{CP,(1)}} - \omega_{\text{anal}}^{\text{LR,(1)}}$ is always positive, showing that the LR result is always smaller than the CP one for the explored systems.

The two approaches CP and LR, at the UHF level of theory can be compared with the exact FCI results. The results are shown in Figs. 2-4, for the molecules H_2 and H_4 in the linear and rectangular geometry, with the 3-21G basis set⁵⁸. For all cases, the LR results are closer to the FCI ones. The plots also show that, in the non-interacting limit ($\lambda = 0$), the LR formalism coincides with FCI as expected from Eq. (44), while the two approaches differ in the interacting case. In the water example with the STO-3G (Fig. 4)⁵⁷, 6-31G^{60,61}, and cc-pVDZ⁶² basis sets (Fig. 5), the three methods show small discrepancies across the range until λ approaches 1.

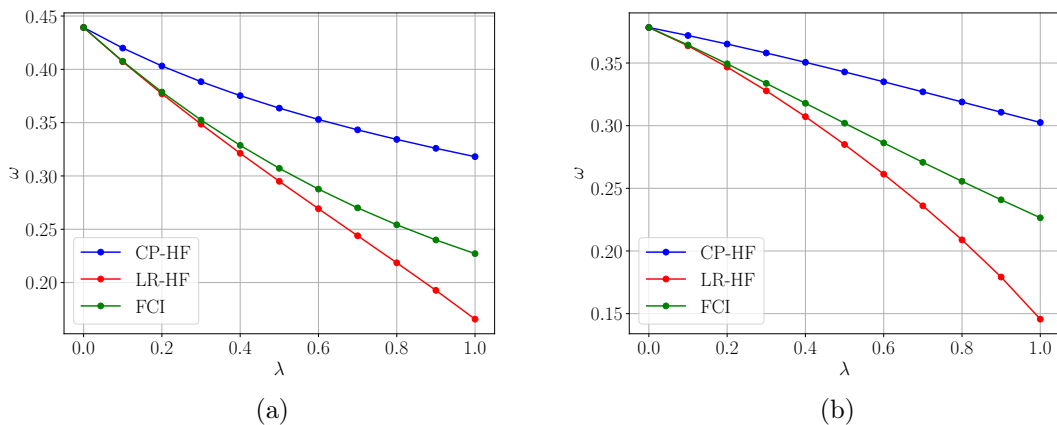


Figure 3: Dependence on the λ -parameter of the excitation energy, calculated on the H_4 molecule, in the linear (a) and rectangular (b) geometries, with the 3-21G basis set.

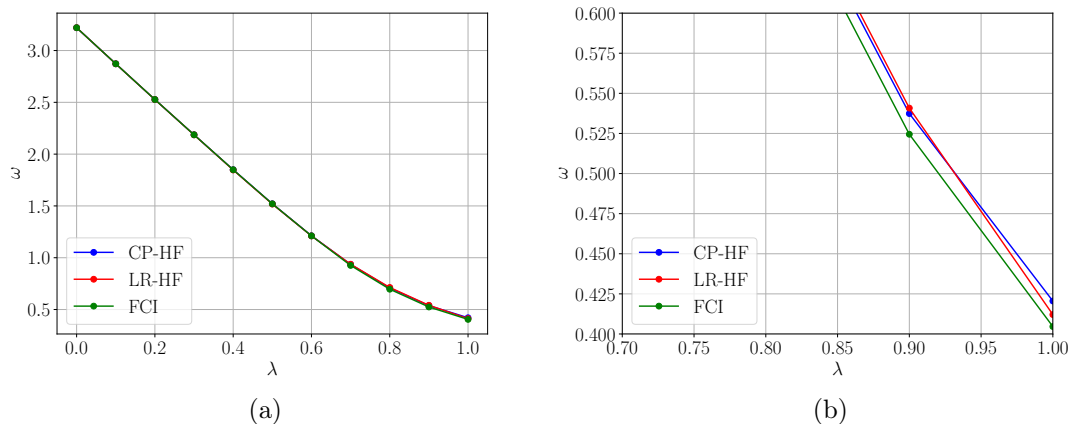


Figure 4: Dependence on the λ -parameter of the excitation energy, calculated on the H_2O , with the STO-3G basis set. In Fig. 4b, a zoom on the differences between the different approaches in the region around $\lambda = 1$ is plotted.

5.2 Multiple critical points within the UHF theory for H_4

Due to the nonlinearities induced by the UHF approximation, there can be multiple critical points (in particular, index-1 saddle points) over the UHF electronic landscape. In this subsection, we consider the H_4 molecule in a rectangular configuration with side lengths of 1 Å and 1.1 Å, at the UHF/STO-3G⁵⁷ level of theory. The Hamiltonian is parametrized by the coupling parameter λ , as in Section 4.1. For each $\lambda \in [0, 2]$ with a spacing of 0.05, we find the index-1 saddle points by running the saddle search algorithm from 50 different randomly generated initial points over the Grassmannian.

Fig. 6 shows the energies of the index-1 saddle points which appear in the range $\lambda \in [0, 2]$. We see that in this range, at most three critical points are found. In the range $\lambda \in [0, 0.35]$, only one index-1 saddle point is found, in $\lambda \in [0.40, 0.60]$ two index-1 saddle points are found, and from there with increasing λ , three index-1 saddle points are observed. At $\lambda \approx 1.68$ the lines corresponding to the second and third saddle points are crossing, showing that the ordering in the energies of the states might not be preserved.

It is known that not all index-1 saddle points provide suitable approximations for

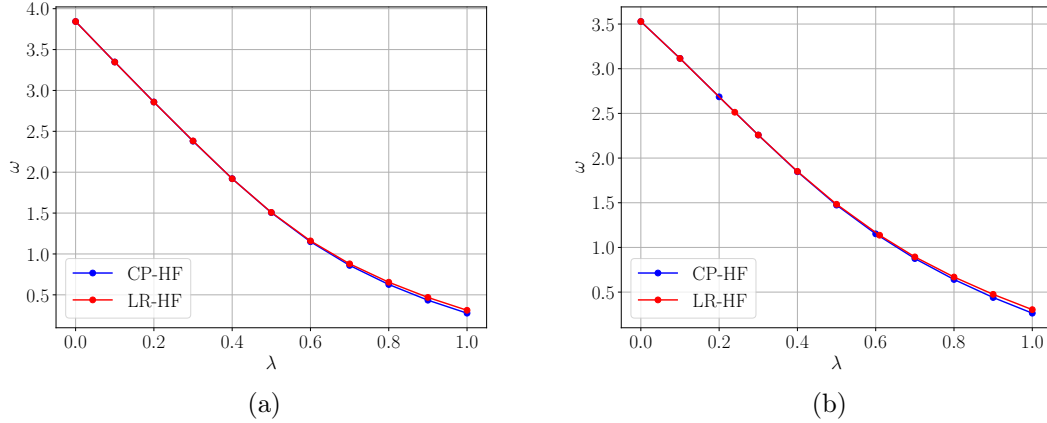


Figure 5: Dependence on the λ -parameter of the excitation energy, calculated on H_2O . In Fig. 5a the 6-31G basis set is used, while in Fig. 5b, the cc-pVDZ basis set is used. At $\lambda = 0.2$ and $\lambda = 0.6$, the TD-HF algorithm in PySCF was not able to converge due to high linear dependencies.

excited states. An interpretation of the critical points can be gained through projection onto the FCI states, as these form a complete basis. Our calculations consider the case of $S_z = 0$, therefore fixing $N_\alpha = N_\beta = 2$. In the present case of a minimal basis set, a total number of 36 FCI states can be built. The projection of the wave functions corresponding to the critical points can be written as

$$|\Psi^{\text{CP-HF}}(\lambda)\rangle = \sum_I c_I(\lambda) |\Psi_I^{\text{FCI}}(\lambda)\rangle.$$

The magnitudes of the $c_I(\lambda)$ coefficients indicate the extent to which the critical points correspond to the I -th FCI state. For the sake of clarity, we will include only the eight lowest-lying FCI states, as the contributions of the higher-energy states are relatively small. We include the evolution of the considered FCI excited energies with the coupling parameter in Fig. 7a. We label these states as $\Psi_0^{\text{FCI}}(\lambda)$, $\Psi_1^{\text{FCI}}(\lambda)$, \dots , $\Psi_7^{\text{FCI}}(\lambda)$ in accordance to their energy ordering in the non-interacting case. At $\lambda = 0$, we observe that the pairs $(\Psi_1^{\text{FCI}}(0), \Psi_2^{\text{FCI}}(0))$, $(\Psi_4^{\text{FCI}}(0), \Psi_5^{\text{FCI}}(0))$, and $(\Psi_6^{\text{FCI}}(0), \Psi_7^{\text{FCI}}(0))$ are degenerate. These degeneracies can be understood by considering the occupation of the molecular orbitals. In the non-interacting case, the lowest eight FCI states are either singlets or triplets and are therefore either single Slater determinants or linear combinations of two Slater determinants:

$$\begin{aligned} |\Psi_0^{\text{FCI}}(0)\rangle &= |\phi_1^\alpha \phi_1^\beta \phi_2^\alpha \phi_2^\beta\rangle \\ (|\Psi_1^{\text{FCI}}(0)\rangle, |\Psi_2^{\text{FCI}}(0)\rangle) &= \frac{1}{\sqrt{2}}(|\phi_1^\alpha \phi_1^\beta \phi_2^\alpha \phi_3^\beta\rangle \pm |\phi_1^\alpha \phi_1^\beta \phi_2^\beta \phi_3^\alpha\rangle) \\ |\Psi_3^{\text{FCI}}(0)\rangle &= |\phi_1^\alpha \phi_1^\beta \phi_3^\alpha \phi_3^\beta\rangle \\ (|\Psi_4^{\text{FCI}}(0)\rangle, |\Psi_5^{\text{FCI}}(0)\rangle) &= \frac{1}{\sqrt{2}}(|\phi_1^\alpha \phi_2^\beta \phi_2^\alpha \phi_3^\beta\rangle \pm |\phi_1^\beta \phi_2^\beta \phi_2^\alpha \phi_3^\alpha\rangle) \\ (|\Psi_6^{\text{FCI}}(0)\rangle, |\Psi_7^{\text{FCI}}(0)\rangle) &= \frac{1}{\sqrt{2}}(|\phi_1^\alpha \phi_1^\beta \phi_2^\alpha \phi_4^\beta\rangle \pm |\phi_1^\alpha \phi_1^\beta \phi_2^\beta \phi_4^\alpha\rangle) \end{aligned}$$

The degeneracies arise from the fact that at $\lambda = 0$, the singlet state and the triplet state of $S_z = 0$ have the same energy, as discussed in Section 4.1.

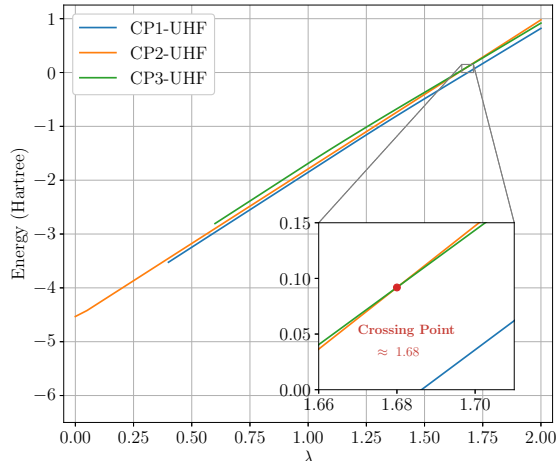


Figure 6: Dependence on the λ -parameter of the energy of the index-1 saddle points, calculated on H_4 in a rectangular configuration with sides of 1 Å and 1.1 Å. The UHF/STO-3G level of theory has been used. Calculations have been made in steps of $\Delta\lambda = 0.2$.

For $\lambda > 0$, it can be observed that the degeneracy is lifted, as the singlet and triplet states no longer give the same energy. With increasing interaction parameter λ , the FCI states are observed to cross. In particular, Ψ_2^{FCI} (green line in Fig. 7a) crosses consecutively with the states Ψ_3^{FCI} , Ψ_4^{FCI} , Ψ_5^{FCI} , Ψ_6^{FCI} (respectively, red, purple, brown, and pink lines in Fig. 7a) at $\lambda \approx 0.77$, 1.33, 1.49, and 1.94 respectively, as indicated by the dot, square, star, and diamond markers in the figure.

In Figs. 7b-7d, the c_I coefficients corresponding to the three index-1 saddle points are plotted. In Fig. 7b, the analysis is performed for the lowest-lying critical point (CP1, blue line in Fig. 6). This saddle point appears only from $\lambda \approx 0.4$ and shows to be dominated by the FCI ground state. Therefore, this critical point can be interpreted as a spurious saddle point arising from the use of an approximate wave function method (UHF), which introduces nonlinearities. The existence of spurious critical points in nonlinear approximation models has been reported many times since the early days of quantum chemistry, and the study of this phenomenon is still an active field of research (cf. e.g., the recent work by Marie and Burton in Ref.⁷ on CASSCF). Fig. 7c shows the same analysis for the second critical point (CP2, orange line in Fig. 6). This state remains a combination of Ψ_1^{FCI} and Ψ_2^{FCI} . In particular, at $\lambda = 0$, we have $|\Psi_2^{\text{HF,CP}}(0)\rangle = \frac{1}{\sqrt{2}}(|\Psi_1^{\text{FCI}}(0)\rangle + |\Psi_2^{\text{FCI}}(0)\rangle)$ at $\lambda = 0$. As the two states Ψ_1^{FCI} and Ψ_2^{FCI} are degenerate at $\lambda = 0$ but belong to different spin-symmetry sectors, this critical point is a symmetry-broken solution, formed by a linear combination of the singlet first excited state Ψ_1^{FCI} and the triplet ground state Ψ_2^{FCI} .

In Fig. 7d, the overlap of the third critical point (CP3, green line in Fig. 6) is shown. It is observed that this critical point, which arises only from $\lambda = 0.60$, has a large overlap with the state Ψ_3^{FCI} . In particular, for $\lambda \in [0.60, 1]$ the overlap is very close to one, but then the saddle point becomes a linear combination of states Ψ_3^{FCI} and Ψ_5^{FCI} .

The analysis confirms once more that the interpretation of critical points as excited states should therefore be performed with care. On the reported example, only one critical point of a Morse index 1 (CP2 in Fig. 6) can be interpreted as a proper approximation of the first excited state in the UHF setting, while the other two are spurious states arising from the intrinsic nonlinearity of the UHF theory.

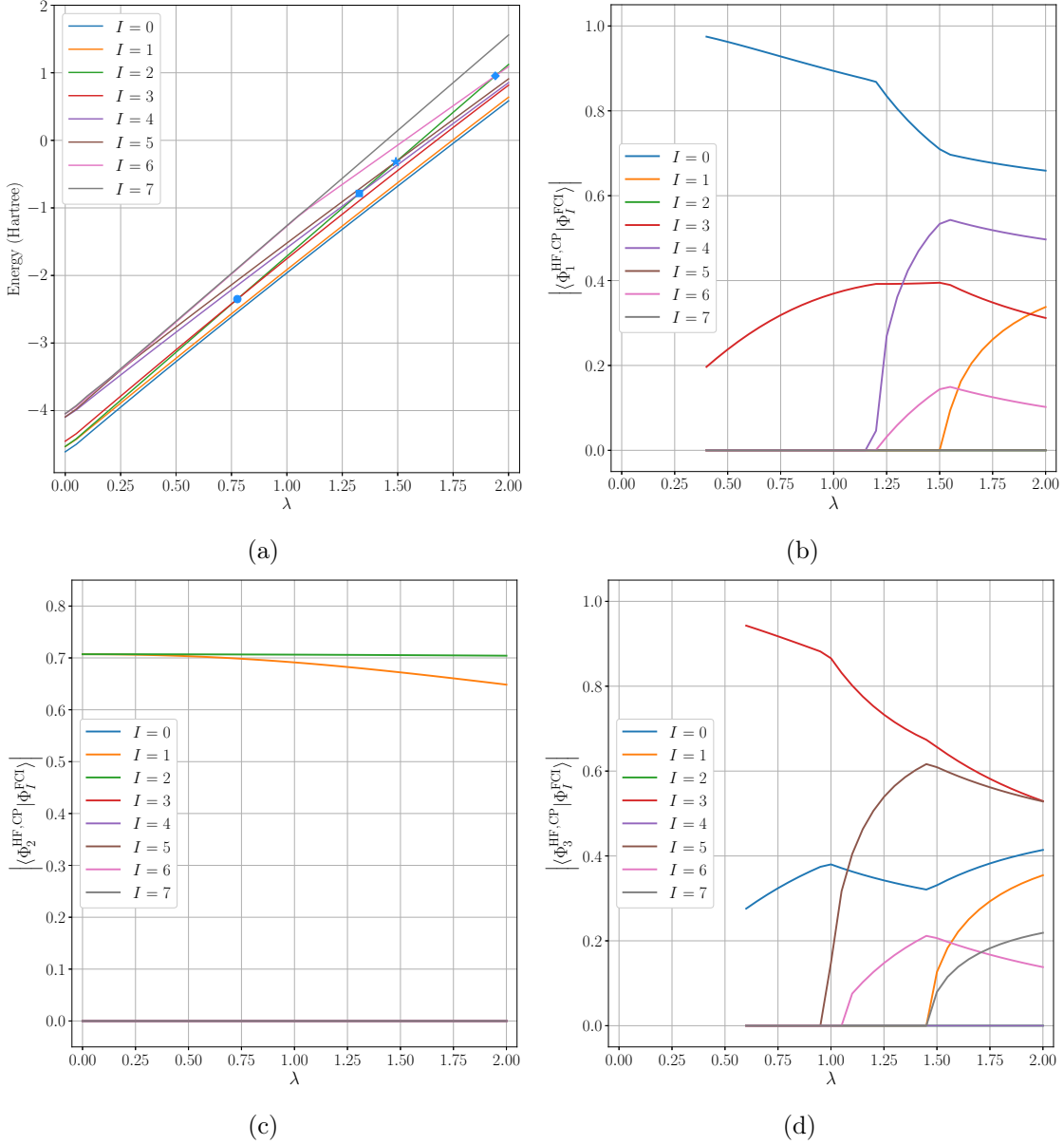


Figure 7: (a) Dependence on the λ -parameter of the FCI energies, and (b-d) dependence on the λ -parameter of the overlaps of the UHF critical points with the FCI states, calculated on H_4 in a rectangular configuration with sides of 1 Å and 1.1 Å. Calculations have been made in steps of $\Delta\lambda = 0.05$.

Acknowledgments

This project has received funding from the European Research Council (ERC) under the European Union’s Horizon 2020 research and innovation programme (grant agreement EMC2 No 810367). This work has benefited from French State support managed by ANR under the France 2030 program through the MaQui CNRS Risky and High-Impact Research programme (RI)² (grant agreement ANR-24-RRII-0001). The authors are grateful to Théo Duez, Asbjörn Lauritsen, Tony Lelièvre, Mathieu Lewin, Filippo Lipparini, Tommaso Nottoli, Panos Parpas, Julien Toulouse, and Jari van Gog for useful discussions.

References

- [1] Leticia González, Daniel Escudero, and Luis Serrano–Andrés. Progress and challenges in the calculation of electronic excited states. *ChemPhysChem*, 13(1): 28–51, September 2011. ISSN 1439-7641. doi: 10.1002/cphc.201100200. URL <http://dx.doi.org/10.1002/cphc.201100200>.
- [2] Kate K. Docken and Juergen Hinze. LiH Potential Curves and Wavefunctions for X $^1\Sigma^+$, A $^1\Sigma^+$, B $^1\Pi$, $^3\Sigma^+$, and $^3\Pi$. *J. Chem. Phys.*, 57(11): 4928–4936, December 1972. ISSN 1089-7690. doi: 10.1063/1.1678164. URL <http://dx.doi.org/10.1063/1.1678164>.
- [3] *State-Specific Theory of Electron Correlation in Excited States*. ISBN 9789400964518.
- [4] K. Hirao. State-specific multireference möller–plesset perturbation treatment for singlet and triplet excited states, ionized states and electron attached states of h₂o. *Chem. Phys. Lett.*, 201(1–4):59–66, January 1993. ISSN 0009-2614. doi: 10.1016/0009-2614(93)85034-l. URL [http://dx.doi.org/10.1016/0009-2614\(93\)85034-l](http://dx.doi.org/10.1016/0009-2614(93)85034-l).
- [5] Fábris Kossoski, Antoine Marie, Anthony Scemama, Michel Caffarel, and Pierre-François Loos. Excited states from state-specific orbital-optimized pair coupled cluster. *J. Chem. Theory Comput.*, 17(8):4756–4768, July 2021. ISSN 1549-9626. doi: 10.1021/acs.jctc.1c00348. URL <http://dx.doi.org/10.1021/acs.jctc.1c00348>.
- [6] Fábris Kossoski and Pierre-François Loos. State-specific configuration interaction for excited states. *J. Chem. Theory Comput.*, 19(8):2258–2269, April 2023. ISSN 1549-9626. doi: 10.1021/acs.jctc.3c00057. URL <http://dx.doi.org/10.1021/acs.jctc.3c00057>.
- [7] Antoine Marie and Hugh G. A. Burton. Excited states, symmetry breaking, and unphysical solutions in state-specific CASSCF theory. *J. Phys. Chem. A*, 127(20): 4538–4552, May 2023. ISSN 1520-5215. doi: 10.1021/acs.jpca.3c00603. URL <http://dx.doi.org/10.1021/acs.jpca.3c00603>.
- [8] Sandra Saade and Hugh G. A. Burton. Excited state-specific CASSCF theory for the torsion of ethylene. *J. Chem. Theory Comput.*, 20(12): 5105–5114, June 2024. ISSN 1549-9626. doi: 10.1021/acs.jctc.4c00212. URL <http://dx.doi.org/10.1021/acs.jctc.4c00212>.
- [9] Poul Jørgensen and Jan Linderberg. Time-dependent Hartree–Fock calculations in the Pariser–Parr–Pople model. Applications to aniline, azulene and pyridine. *Int. J. Quantum Chem.*, 4(6):587–602, November 1970. ISSN 1097-461X. doi: 10.1002/qua.560040606. URL <http://dx.doi.org/10.1002/qua.560040606>.
- [10] Jeppe Olsen, Hans Jørgen Aa Jensen, and Poul Jørgensen. Solution of the large matrix equations which occur in response theory. *J. Comput. Phys.*, 74(2): 265–282, February 1988. ISSN 0021-9991. doi: 10.1016/0021-9991(88)90081-2. URL [http://dx.doi.org/10.1016/0021-9991\(88\)90081-2](http://dx.doi.org/10.1016/0021-9991(88)90081-2).
- [11] E. Dalgaard. Quadratic response functions within the time-dependent Hartree–Fock approximation. *Phys. Rev. A*, 26(1):42–52, July 1982. ISSN 0556-2791. doi: 10.1103/physreva.26.42. URL <http://dx.doi.org/10.1103/PhysRevA.26.42>.

- [12] Masayuki Matsuo. Continuum linear response in coordinate space Hartree–Fock–Bogoliubov formalism for collective excitations in drip-line nuclei. *Nucl. Phys. A*, 696(3–4):371–395, December 2001. ISSN 0375-9474. doi: 10.1016/s0375-9474(01)01133-2. URL [http://dx.doi.org/10.1016/S0375-9474\(01\)01133-2](http://dx.doi.org/10.1016/S0375-9474(01)01133-2).
- [13] Shuichiro Ebata, Takashi Nakatsukasa, Tsunenori Inakura, Kenichi Yoshida, Yukio Hashimoto, and Kazuhiro Yabana. Canonical-basis time-dependent Hartree-Fock-Bogoliubov theory and linear-response calculations. *Phys. Rev. C*, 82(3):034306, September 2010. ISSN 1089-490X. doi: 10.1103/physrevc.82.034306. URL <http://dx.doi.org/10.1103/PhysRevC.82.034306>.
- [14] Masanori Miura and Yuriko Aoki. Linear-scaled excited state calculations at linear response time-dependent Hartree–Fock theory. *Mol. Phys*, 108(2):205–210, January 2010. ISSN 1362-3028. doi: 10.1080/00268971003596169. URL <http://dx.doi.org/10.1080/00268971003596169>.
- [15] R. van Meer, O. V. Gritsenko, and E. J. Baerends. Natural excitation orbitals from linear response theories: Time-dependent density functional theory, time-dependent Hartree-Fock, and time-dependent natural orbital functional theory. *J. Chem. Phys.*, 146(4):044119, January 2017. ISSN 1089-7690. doi: 10.1063/1.4974327. URL <http://dx.doi.org/10.1063/1.4974327>.
- [16] Robert Berger and Martin Quack. Multiconfiguration linear response approach to the calculation of parity violating potentials in polyatomic molecules. *J. Chem. Phys.*, 112(7):3148–3158, February 2000. ISSN 1089-7690. doi: 10.1063/1.480900. URL <http://dx.doi.org/10.1063/1.480900>.
- [17] Jonna Stålring, Anders Bernhardsson, and Per-Åke Malmqvist. A linear response approach to second-order electronic transition intensities for multiconfigurational self-consistent field wave functions. *J. Chem. Phys.*, 117(3):1010–1016, July 2002. ISSN 1089-7690. doi: 10.1063/1.1485724. URL <http://dx.doi.org/10.1063/1.1485724>.
- [18] Benjamin Helmich-Paris. Benchmarks for electronically excited states with CASSCF methods. *J. Chem. Theory Comput.*, 15(7):4170–4179, May 2019. ISSN 1549-9626. doi: 10.1021/acs.jctc.9b00325. URL <http://dx.doi.org/10.1021/acs.jctc.9b00325>.
- [19] Benjamin Helmich-Paris. CASSCF linear response calculations for large open-shell molecules. *J. Chem. Phys.*, 150(17):174121, May 2019. ISSN 1089-7690. doi: 10.1063/1.5092613. URL <http://dx.doi.org/10.1063/1.5092613>.
- [20] Erich Runge and E. K. U. Gross. Density-functional theory for time-dependent systems. *Phys. Rev. Lett*, 52(12):997–1000, March 1984. ISSN 0031-9007. doi: 10.1103/physrevlett.52.997. URL <http://dx.doi.org/10.1103/PhysRevLett.52.997>.
- [21] E. K. U. Gross and Walter Kohn. Local density-functional theory of frequency-dependent linear response. *Phys. Rev. Lett*, 55(26):2850–2852, December 1985. ISSN 0031-9007. doi: 10.1103/physrevlett.55.2850. URL <http://dx.doi.org/10.1103/PhysRevLett.55.2850>.
- [22] Giovanni Onida, Lucia Reining, and Angel Rubio. Electronic excitations: density-functional versus many-body green’s-function approaches. *Rev. Mod. Phys.*, 74(2):601–659, June 2002. ISSN 1539-0756. doi: 10.1103/revmodphys.74.601. URL <http://dx.doi.org/10.1103/RevModPhys.74.601>.

- [23] *Time-Dependent Density Functional Response Theory for Molecules.*
- [24] Mark E. Casida, Christine Jamorski, Kim C. Casida, and Dennis R. Salahub. Molecular excitation energies to high-lying bound states from time-dependent density-functional response theory: Characterization and correction of the time-dependent local density approximation ionization threshold. *J. Chem. Phys.*, 108(11):4439–4449, March 1998. ISSN 1089-7690. doi: 10.1063/1.475855. URL <http://dx.doi.org/10.1063/1.475855>.
- [25] Mark E. Casida. Propagator corrections to adiabatic time-dependent density-functional theory linear response theory. *J. Chem. Phys.*, 122(5):054111, January 2005. ISSN 1089-7690. doi: 10.1063/1.1836757. URL <http://dx.doi.org/10.1063/1.1836757>.
- [26] D. Mukherjee and P.K. Mukherjee. A response-function approach to the direct calculation of the transition-energy in a multiple-cluster expansion formalism. *J. Chem. Phys.*, 39(3):325–335, June 1979. ISSN 0301-0104. doi: 10.1016/0301-0104(79)80153-6. URL [http://dx.doi.org/10.1016/0301-0104\(79\)80153-6](http://dx.doi.org/10.1016/0301-0104(79)80153-6).
- [27] Hideo Sekino and Rodney J. Bartlett. A linear response, coupled-cluster theory for excitation energy. *Int. J. Quantum Chem.*, 26(S18):255–265, March 1984. ISSN 1097-461X. doi: 10.1002/qua.560260826. URL <http://dx.doi.org/10.1002/qua.560260826>.
- [28] Marcel Nooijen and Rodney J. Bartlett. Equation of motion coupled cluster method for electron attachment. *J. Chem. Phys.*, 102(9):3629–3647, March 1995. ISSN 1089-7690. doi: 10.1063/1.468592. URL <http://dx.doi.org/10.1063/1.468592>.
- [29] Marcel Nooijen and Rodney J. Bartlett. Similarity transformed equation-of-motion coupled-cluster theory: Details, examples, and comparisons. *J. Chem. Phys.*, 107(17):6812–6830, November 1997. ISSN 1089-7690. doi: 10.1063/1.474922. URL <http://dx.doi.org/10.1063/1.474922>.
- [30] Marcel Nooijen and Rodney J. Bartlett. A new method for excited states: Similarity transformed equation-of-motion coupled-cluster theory. *J. Chem. Phys.*, 106(15):6441–6448, April 1997. ISSN 1089-7690. doi: 10.1063/1.474000. URL <http://dx.doi.org/10.1063/1.474000>.
- [31] Jan Geertsen, Magnus Rittby, and Rodney J. Bartlett. The equation-of-motion coupled-cluster method: Excitation energies of be and co. *Chem. Phys. Lett.*, 164(1):57–62, December 1989. ISSN 0009-2614. doi: 10.1016/0009-2614(89)85202-9. URL [http://dx.doi.org/10.1016/0009-2614\(89\)85202-9](http://dx.doi.org/10.1016/0009-2614(89)85202-9).
- [32] John F. Stanton and Rodney J. Bartlett. The equation of motion coupled-cluster method. a systematic biorthogonal approach to molecular excitation energies, transition probabilities, and excited state properties. *J. Chem. Phys.*, 98(9):7029–7039, May 1993. ISSN 1089-7690. doi: 10.1063/1.464746. URL <http://dx.doi.org/10.1063/1.464746>.
- [33] Henrik Koch and Poul Jørgensen. Coupled cluster response functions. *J. Chem. Phys.*, 93(5):3333–3344, 1990.
- [34] Donald C. Comeau and Rodney J. Bartlett. The equation-of-motion coupled-cluster method. applications to open- and closed-shell reference states. *Chem. Phys. Lett.*,

- 207(4–6):414–423, May 1993. ISSN 0009-2614. doi: 10.1016/0009-2614(93)89023-b. URL [http://dx.doi.org/10.1016/0009-2614\(93\)89023-B](http://dx.doi.org/10.1016/0009-2614(93)89023-B).
- [35] P.J. Knowles and N.C. Handy. A new determinant-based full configuration interaction method. *Chem. Phys. Lett.*, 111(4–5):315–321, November 1984. ISSN 0009-2614. doi: 10.1016/0009-2614(84)85513-x. URL [http://dx.doi.org/10.1016/0009-2614\(84\)85513-X](http://dx.doi.org/10.1016/0009-2614(84)85513-X).
- [36] Jeppe Olsen, Poul Jørgensen, and Jack Simons. Passing the one-billion limit in full configuration-interaction (FCI) calculations. *Chem. Phys. Lett.*, 169(6):463–472, June 1990. ISSN 0009-2614. doi: 10.1016/0009-2614(90)85633-n. URL [http://dx.doi.org/10.1016/0009-2614\(90\)85633-N](http://dx.doi.org/10.1016/0009-2614(90)85633-N).
- [37] Miguel AL Marques, Carsten A Ulrich, Fernando Nogueira, Angel Rubio, Kieron Burke, and Eberhard KU Gross. *Time-dependent Density Functional Theory*, volume 706. Springer, 2006.
- [38] Miguel AL Marques, Neepa T Maitra, Fernando MS Nogueira, Eberhard KU Gross, and Angel Rubio. *Fundamentals of time-dependent density functional theory*, volume 837. Springer, 2012.
- [39] Björn O. Roos, Peter R. Taylor, and Per E.M. Sigbahn. A complete active space scf method (casscf) using a density matrix formulated super-ci approach. *Chem. Phys.*, 48(2):157–173, May 1980. ISSN 0301-0104. doi: 10.1016/0301-0104(80)80045-0. URL [http://dx.doi.org/10.1016/0301-0104\(80\)80045-0](http://dx.doi.org/10.1016/0301-0104(80)80045-0).
- [40] J Cizek and J Paldus. Coupled cluster approach. *Phys. Scr.*, 21(3–4):251–254, January 1980. ISSN 1402-4896. doi: 10.1088/0031-8949/21/3-4/006. URL <http://dx.doi.org/10.1088/0031-8949/21/3-4/006>.
- [41] J. Cizek. Origins of coupled cluster technique for atoms and molecules. *Theor. Chim. Acta*, 80(2–3):91–94, March 1991. ISSN 1432-2234. doi: 10.1007/bf01119616. URL <http://dx.doi.org/10.1007/BF01119616>.
- [42] Rodney J. Bartlett and Monika Musiał. Coupled-cluster theory in quantum chemistry. *Rev. Mod. Phys.*, 79(1):291–352, February 2007. ISSN 1539-0756. doi: 10.1103/revmodphys.79.291. URL <http://dx.doi.org/10.1103/RevModPhys.79.291>.
- [43] M. Lewin. Solutions of the multiconfiguration equations in quantum chemistry. *Arch. Ration. Mech. Anal.*, 171:83–114, 2004. doi: 10.1007/s00205-003-0281-6.
- [44] E. Cancès, H. Galicher, and M. Lewin. Computing electronic structures: A new multiconfiguration approach for excited states. *J. Comput. Phys.*, 212(1):73–98, 2006. doi: 10.1016/j.jcp.2005.06.015.
- [45] D. Huybrechts. *Complex Geometry: An Introduction*, volume 78 of *Universitext*. Springer Berlin, Heidelberg, 2005. doi: 10.1007/b137952.
- [46] Andrei Moroianu. *Lectures on Kähler Geometry*. London Mathematical Society Student Texts. Cambridge University Press, 2007.
- [47] R. O. Wells. *Differential Analysis on Complex Manifolds*, volume 65 of *Graduate Texts in Mathematics*. Springer New York, NY, third edition, 2008. doi: 10.1007/978-0-387-73892-5.

- [48] J. Williamson. On the algebraic problem concerning the normal forms of linear dynamical systems. *Am. J. Math.*, 58(1):141–163, 1936. doi: 10.2307/2371062.
- [49] T. Bendokat, R. Zimmermann, and P.-A. Absil. A grassmann manifold handbook: Basic geometry and computational aspects. *Adv. Comput. Math.*, 50(1):6, 2024. doi: 10.1007/s10444-023-10090-8.
- [50] A. Edelman, T. A. Arias, and S. T. Smith. The geometry of algorithms with orthogonality constraints. *SIAM J. Matrix Anal. Appl.*, 20(2):303–353, 1998. doi: 10.1137/S0895479895290954.
- [51] P.-A. Absil, R. Mahony, and R. Sepulchre. *Optimization Algorithms on Matrix Manifolds*. Princeton University Press, Princeton, NJ, 2008. doi: 10.1515/9781400830244.
- [52] N. Boumal. *An Introduction to Optimization on Smooth Manifolds*. Cambridge University Press, 2023. doi: 10.1017/9781009166164.
- [53] T. Helgaker, P. Jørgensen, and J. Olsen. *Molecular Electronic-Structure Theory*. John Wiley & Sons, Ltd, 2000. ISBN 9781119019572. doi: 10.1002/9781119019572.
- [54] Volker Bach, Elliott H. Lieb, Michael Loss, and Jan Philip Solovej. There are no unfilled shells in unrestricted Hartree-Fock theory. *Phys. Rev. Lett.*, 72(19):2981–2983, May 1994. doi: 10.1103/PhysRevLett.72.2981.
- [55] Mark E. Casida. Time-dependent density-functional theory for molecules and molecular solids. *J. Mol. Struct. THEOCHEM*, 914(1):3–18, 2009. ISSN 0166-1280. doi: <https://doi.org/10.1016/j.theochem.2009.08.018>. URL <https://www.sciencedirect.com/science/article/pii/S0166128009005363>.
- [56] Qiming Sun, Xing Zhang, Samragni Banerjee, Peng Bao, Marc Barbry, Nick S. Blunt, Nikolay A. Bogdanov, George H. Booth, Jia Chen, Zhi-Hao Cui, Janus J. Eriksen, Yang Gao, Sheng Guo, Jan Hermann, Matthew R. Hermes, Kevin Koh, Peter Koval, Susi Lehtola, Zhendong Li, Junzi Liu, Narbe Mardirossian, James D. McClain, Mario Motta, Bastien Mussard, Hung Q. Pham, Artem Pulkin, Wirawan Purwanto, Paul J. Robinson, Enrico Ronca, Elvira R. Sayfutyarova, Maximilian Scheurer, Henry F. Schurkus, James E. T. Smith, Chong Sun, Shi-Ning Sun, Shiv Upadhyay, Lucas K. Wagner, Xiao Wang, Alec White, James Daniel Whitfield, Mark J. Williamson, Sebastian Wouters, Jun Yang, Jason M. Yu, Tianyu Zhu, Timothy C. Berkelbach, Sandeep Sharma, Alexander Yu. Sokolov, and Garnet Kin-Lic Chan. Recent developments in the PySCF program package. *J. Chem. Phys.*, 153(2), July 2020. ISSN 1089-7690.
- [57] W. J. Hehre, R. F. Stewart, and J. A. Pople. Self-consistent molecular-orbital methods. i. use of gaussian expansions of slater-type atomic orbitals. *J. Chem. Phys.*, 51:2657–2664, 1969. doi: 10.1063/1.1672392.
- [58] J. Stephen Binkley, John A. Pople, and Warren J. Hehre. Self-consistent molecular orbital methods. 21. small split-valence basis sets for first-row elements. *J. Am. Chem. Soc.*, 102:939–947, 1980. doi: 10.1021/ja00523a008.
- [59] H. G. A. Burton and D. J. Wales. Energy landscapes for electronic structure. *J. Chem. Theory Comput.*, 17(1):151–169, 2020. doi: 10.1021/acs.jctc.0c00772.
- [60] R. Ditchfield, W. J. Hehre, and J. A. Pople. Self-consistent molecular-orbital methods. ix. an extended gaussian-type basis for molecular-orbital studies of organic molecules. *J. Chem. Phys.*, 54:724–728, 1971. doi: 10.1063/1.1674902.

- [61] W. J. Hehre, R. Ditchfield, and J. A. Pople. Self-consistent molecular orbital methods. xii. further extensions of gaussian-type basis sets for use in molecular orbital studies of organic molecules. *J. Chem. Phys.*, 56:2257–2261, 1972. doi: 10.1063/1.1677527.
- [62] Thom H. Dunning. Gaussian basis sets for use in correlated molecular calculations. i. the atoms boron through neon and hydrogen. *J. Chem. Phys.*, 90:1007–1023, 1989. doi: 10.1063/1.456153.